Geometry Mismatch and Reticular Chemistry: Strategies To Assemble Metal–Organic Frameworks with Non-default Topologies

Vincent Guillerm, Daniel Maspoch

Geometry mismatch and reticular chemistry: strategies to assemble metal-organic frameworks with non-default topologies

Vincent Guillerm†* and Daniel Maspoch†‡*

† Catalan Institute of Nanoscience and Nanotechnology (ICN2), CSIC and The Barcelona Institute of Science and Technology, Campus UAB, Bellaterra, 08193 Barcelona, Spain

‡. ICREA, Pg. Lluís Companys 23, 08010 Barcelona, Spain

KEYWORDS. metal-organic frameworks, reticular chemistry, rational design, geometry mismatch, self-assembly, porous materials.

ABSTRACT

The past 20 years have witnessed tremendous advances in the field of porous materials, including the development of novel metal-organic frameworks (MOFs) that show great potential for practical applications aimed at addressing global environmental and industrial challenges. A critical tool enabling this progress has been *reticular chemistry*, through which researchers can design materials that exhibit highly regular (*i.e.* edge-transitive) topologies, based on the assembly of geometrically-matched building blocks into specific nets. However, innovation sometimes demands that researchers steer away from default topologies to instead pursue unusual geometries. In this review, we cover this aspect and introduce the concept of *geometry mismatch*, in which seemingly incompatible building blocks are combined to generate non-default structures. We describe diverse MOF assemblies built through geometry mismatch generated by use of ligand bend-angles, twisted functional groups, zigzag ligands and other elements, focusing on carboxylate-based MOFs combined with common inorganic clusters. We aim to provide a fresh perspective on rational design of MOFs and to help readers understand the countless options now available to achieve greater structural complexity in MOFs.

1. Introduction

Since the consecutive discovery of HKUST-1[1] and MOF-5[2] some 20 years ago, great efforts have been dedicated to understanding the basic principles that govern MOF assembly.[3] The final structure of a given MOF is now widely understood to be strongly influenced by the geometries of its constituent organic ligands and inorganic moieties (*e.g.* single metal ions, polynuclear clusters, infinite chains, *etc.*). Numerous design approaches such as use of molecular building blocks (MBBs) or secondary building units (SBUs) [4-10] have been combined with the mathematic discipline of topology[11-13] to synthesize myriad novel porous structures,[14] including MOFs that exhibit high performance in crucial environmental and industrial applications such as energy/gas storage separation,[15-18] waste/valuables removal,[19, 20] water harvesting[21-25] and smart materials.[26-28]

Concerted efforts by chemists and materials scientists have given rise to a new subfield of chemistry: *reticular chemistry*. The dedicated Reticular Chemistry Structure Resource (RCSR) database created in 2008 by O'Keeffe and coworkers now contains roughly 3,000 three-periodic nets (topologies).[29] One might imagine that there would be a limited number of ways to periodically assemble polygons and polyhedra and that all of these structures would have already been predicted. Surprisingly, this is not the case, even though there are already almost 100,000 MOF structures reported in the MOF subset of the Cambridge structural database.[30] Indeed, there are near-monthly reports of MOFs that exhibit topologies described as "novel", "previously unknown", "unprecedented" or "unique". For instance, Jiang *et al.* discovered more than 120 novel topologies,[31] called *merged nets*.[9] Each of these has minimal transitivity, resulting from the merging of compatible nets. However, reticular chemistry is not limited to the discovery of novel 3D periodic nets: in fact, researchers have often discovered MOFs whose constituent clusters have never previously been reported as discrete molecules. Some of these clusters have high connectivity, which is a highly desired asset.[32-35] Indeed, the greater the connectivity within the building blocks, the lower number of possible structures attainable upon assembly and consequently, the lesser the chance of obtaining an undesired structure. For example, squares[36, 37] or tetrahedra can assemble into numerous structures (248 zeolitic nets known),[38] whereas triangles and rhombicuboctaedra (**rco**) can only assemble into one net the **rht** topology.[39] Accordingly, researchers have been seeking MBBs[10, 32, 34, 40-46] or supermolecular building blocks (SBBs)[4, 32, 39, 47, 48] of high connectivity, with which to rationally construct MOFs. However, whereas most efforts are focused on joining together compatible building blocks to form MOFs of predicable structures and topologies, an opposite

strategy would be to combine apparently incompatible building blocks into structures and topologies, which would provide an opportunity to learn about their behavior and access unprecedented materials.[32] Along these lines, scientists can employ less-symmetric organic ligands, with bend-angles,[34] introduce steric hindrance[49] or use zigzag-shaped ligands (transversal reticular chemistry).[50] These strategies all induce structural irregularity known as *geometry mismatch.*

Theoretically, geometry mismatch could be harnessed for any class of MOFs, such as azolated or phosphonated MOFs. However, in this review, we focus on carboxylate-based MOFs combined with common inorganic MBBs (*i.e.* those for which the synthetic conditions are well known). Given their abundance in the Cambridge Structural Database,[51] we consider the following clusters suitable for reliable analysis: M^{II} *(Cu, Zn, Co, etc.) paddle wheels*, as in HKUST-1;[1] M^{III} *(Fe, Cr, Sc, Ga, Al, etc.) trimers*, as in MIL-100;[52] *Zn tetramers*, as in MOF-5;[2] and $M^{III/IV}$ *(rare earths [RE], Zr and Hf) hexamers*, as in UiO-66.[53] Thus, here we describe examples of MOFs and synthetic strategies that have pushed the envelope of reticular chemistry, challenged standard assembly rules and enabled high degrees of structural complexity, all thanks to the geometry mismatch generated through assembly of their (apparently incompatible) respective building blocks.

2. Topological tools in reticular chemistry: a precious but limited asset

2.1. Nets, nodes, augmented nets and vertex figures

In this section, we briefly highlight the role of topology in the standard design strategy for MOF synthesis, endeavoring to help novices understand the potential and limits of topology in structure design and prediction, through the relatively counterintuitive strategies that we describe in this review. In fact, reticular chemistry has always been associated with topology, and several articles from Delgado-Friedrich *et al.* have been a major source of inspiration for molecular architects.[11, 12, 54-57] Targeting a specific MOF requires selection of at least one organic MBB and one inorganic MBB, each of which will have a specific connectivity (*i.e.* the number of other MBBs it will be linked to). Ideally, assembly of these building blocks would be limited to only one possible structure. The resultant three-periodic net should be as regular as possible, preferably edge-transitive (*i.e.* having only one type of edge bridging the nodes of the net), such that the risk of obtaining undesired structures is minimized.

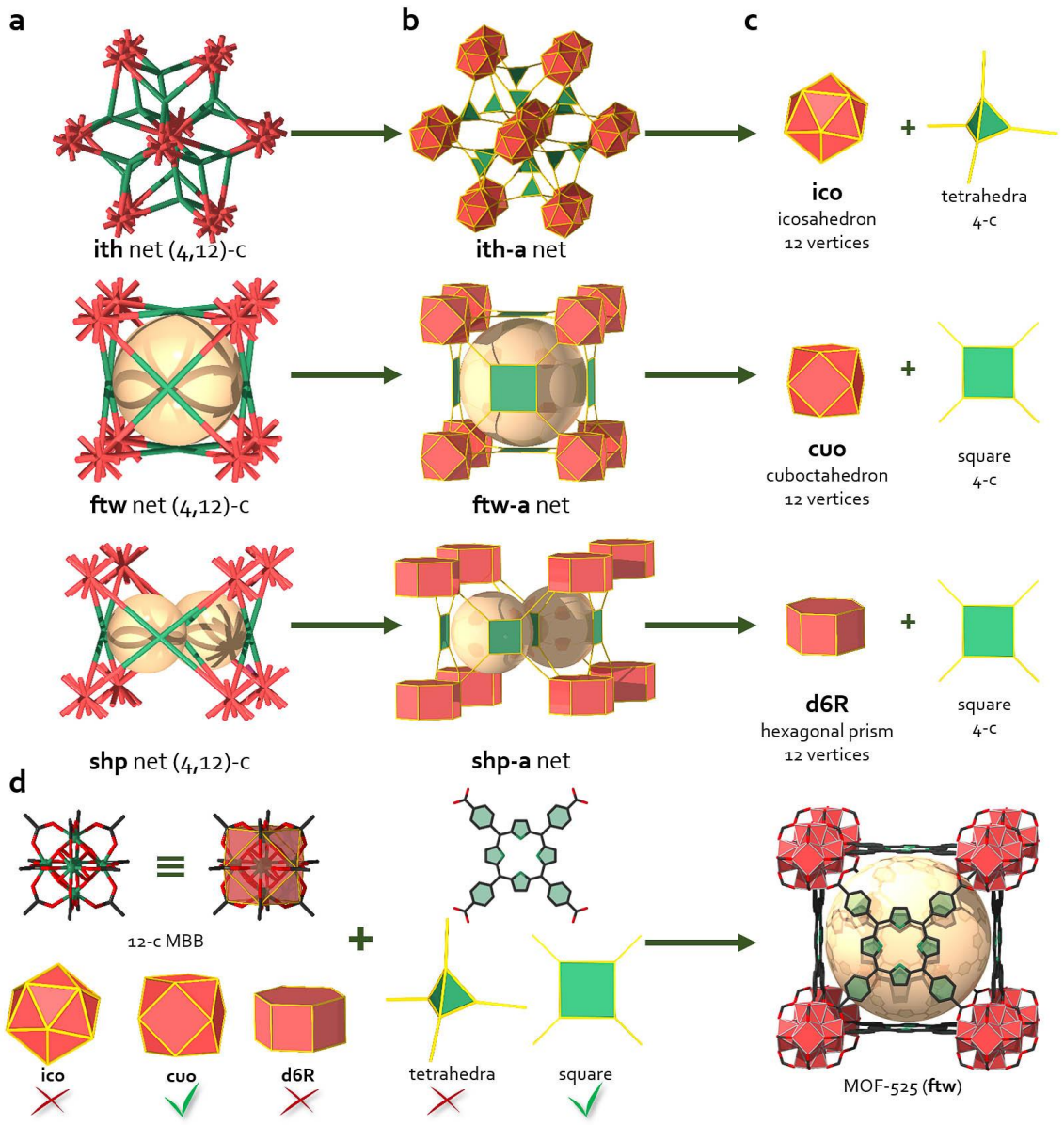

Figure 1 a) The three edge-transitive (4,12)-c nets **ith**, **ftw** and **shp**. b) Augmented representation of the three edge-transitive (4,12)-nets **ith-a**, **ftw-a** and **shp-a**. c) Polygonal and polyhedral building units resulting from the deconstruction of augmented nets. d) Topology prediction map for the assembly of a 12-c hexanuclear cluster with 4-c tcpp ligand, leading to the **ftw**-type structure of MOF-525.

As an illustrative example, we consider the ideally 12-connected (12-c) Zr hexanuclear cluster and the 4-connected ligand, tetrakis(4-carboxyphenyl)porphyrin (tcpp). The expected topology would be an edge-transitive (4,12)-c net. According to the RCSR database, three such nets exist: **ith**, **ftw** and **shp** (Figure 1a). To differentiate among these three nets and find the expected structure, one must inspect the corresponding augmented nets (**net-a,** Figure 1b), in

which the vertices (nodes) are replaced with the corresponding vertex figures (polygons or polyhedra). Such inspection reveals that **ith**, **ftw** and **shp** differ from each other: thus, **ith-a** is the combination of icosahedra with tetrahedra; **ftw-a** comprises cuboctahedra linked by squares; and **shp-a** comprises hexagonal prisms and squares (Figure 1c). In parallel, the twelve extension points of the Zr cluster together form a cuboctahedron, whereas the four extension points of the tcpp ligand form a square. Therefore, formation of the nets **ith** or **shp** can be excluded. Consequently, for a MOF with 12-c Zr cluster and a 4-c tcpp ligand, the expected topology is **ftw** (MOF-525, Figure 1d).[58]

2.2. Angles, offset and twists in organic ligands: limitations of topology in MOF design

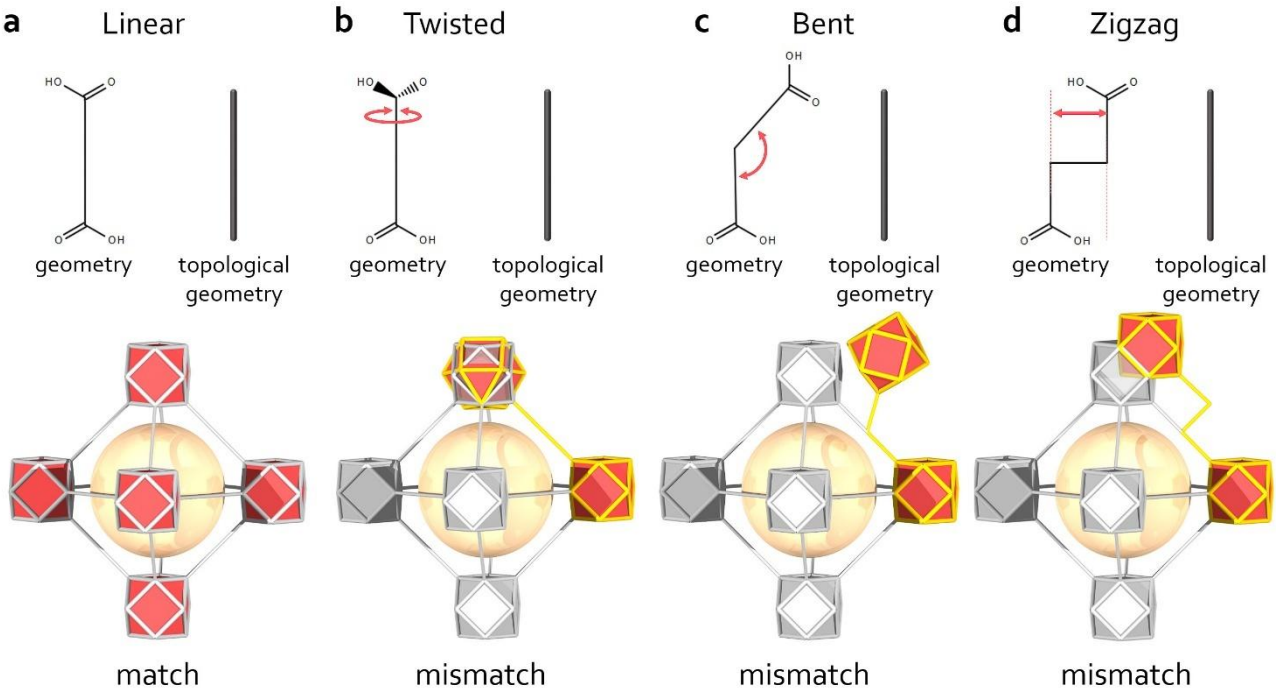

Figure 2. Schematic representation of a) the **fcu-a** net and how b) twisted, c) bent or d) zigzag ligands would create geometry mismatch.

After illustrating (*vide supra*) the prime importance and power of topology as a design tool in reticular chemistry, we address here its relative weakness. Indeed, the simplification of a structure into its underlying net (topology) reduces MBBs as nodes, or for the case of ligands that are 2-connected, it is simply discarded and corresponds to the edges of the net. For instance, UiO-66 comprises 12-c Zr MBBs bridged by 2-c terephthalates; however, the corresponding **fcu** topology is uninodal (12-c net). Therefore, it is difficult to gain insight *a priori* on the possible

effects of different ligand geometries (*i.e.* introducing a twist, an angle or an offset into a 2-c ligand) on the resulting structure or topology, apart from evidence that it might create geometry mismatch and thus, prevent formation of the default structure or topology (Figure 2). In the following sections, we aim to elucidate existing strategies and remaining challenges for the efficient design of MOFs with less regular, non-default topologies.

3. Linear, twisted ligands with steric hindrance: a cornerstone of MOF design

*In this section, the default topologies are the edge-transitive **sql** net (4-c), in the case of 4-c paddle wheels, and **fcu** net (12-c), in the case of Zr/Hf/RE hexanuclear clusters ("UiO type cluster"). Both types of MOFs assemble by bridging linear ligands with coplanar carboxylate groups. Breaking this coplanarity by introducing steric hindrance creates geometry mismatch (Figure 2b).*

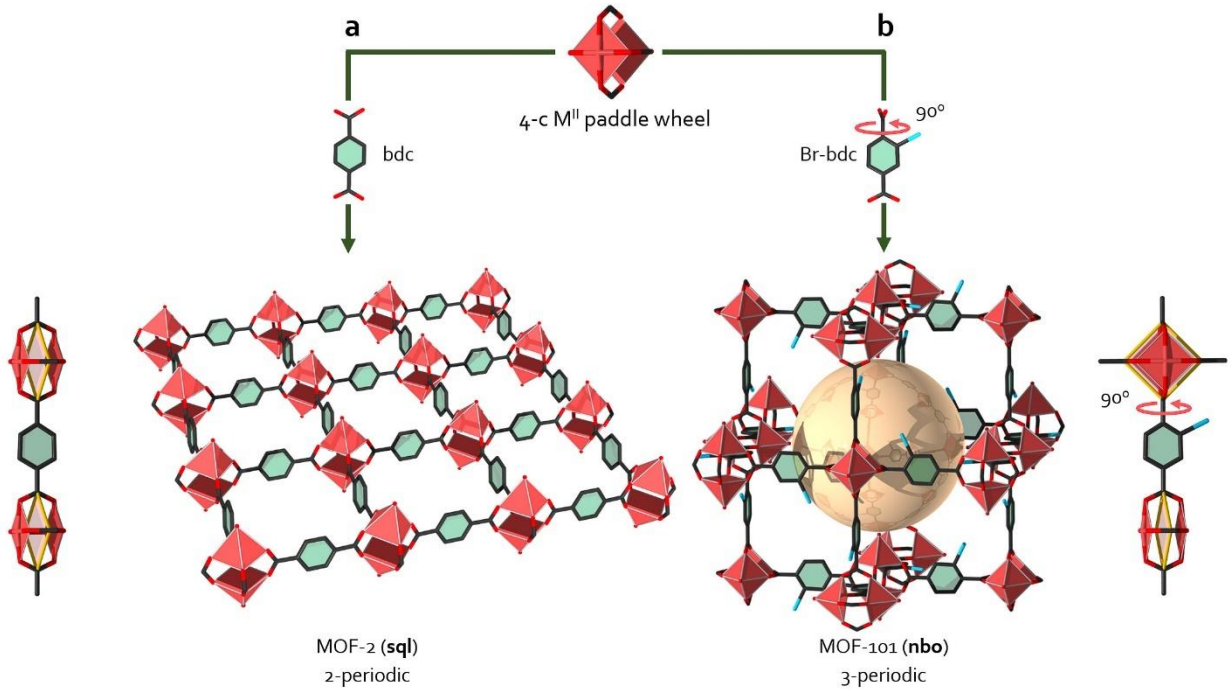

Figure 3. Assembly of bdc or Br-bdc with paddle wheels leads to a) 2-periodic (MOF-2, **sql**) or b) 3-periodic (MOF-101, **nbo**) structures, respectively.

Until 2002, the majority of reported structures resulted from either isoreticular expansion of known MOFs, to create isoreticular MOFs (IRMOFs),[59] or from exploratory trial-and-error work.[1, 60-64] Then, the report of MOF-101, a Cu dicarboxylate, appeared as a cornerstone of rational MOF design in reticular chemistry (Figure 3).[49] To modify the orientation of the Cu paddle wheels, the coplanarity between the two carboxylic groups in the linear

terephthalate (bdc) was broken, by employing a sterically hindered ligand (Br-bdc). This altered the directionality of the connectivity points by 90º, enabling formation of a 3-periodic structure with the **nbo** topology (Figure 3b), rather than the **sql** topology of MOF-2 (Figure 3a).[63] However, the twist angle does not need to be as large as 90º to affect the structure and topology of a MOF. For example, smaller twists in the ligands (28º and 47º) will alter the directionality of the paddle wheels to a lesser extent than in MOF-101. Using this approach, Furukawa *et al.* formed MOF-604, which exhibits the **cds** topology.[36] This strategy has also been applied with longer ligands such as 2,2′-dimethyl biphenyl-4,4′-dicarboxylate (Me_2bpdc)[36] as well as with zirconium, enabling formation of Zr-based MOFs with the **bcu** topology,[65-67] rather than the **fcu** topology, which is commonly obtained when linear ligands are used.[40, 53, 68-71] Lü *et al.* described a surprising example along these lines, having assembled the complex, chiral N,N′-di-(4-benzate)-1,2,6,7-tetrachloroperylene-3,4,9,10-tetracarboxylic acid diimide (pdi) with zirconium. [72] The dihedral angle between the two carboxylates (38°), and the unusual length and slight flexibility of the ligand, together generated the **dia** topology, rather than the **fcu** or **bcu** topologies. In this structure, the Zr clusters of Zr-PDI are capped by eight ligands, such that each cluster is connected to four others (*i.e.* two ligands each bridge two similar clusters). As a concluding example, we consider the zinc tetramer used to produce IRMOFs.[59] Interestingly, unlike in the case of M^{II} paddle wheels (Figure 4a) and $M^{III/IV}$ hexanuclear clusters (Figure 4c), for IRMOFs, introducing a 90º twist into the organic ligands does not have any impact on the resulting connectivity directions of the cluster (Figure 4b). This is due to the octahedral connectivity of the zinc tetramer. To the best of our knowledge, this observation has not been reported elsewhere.

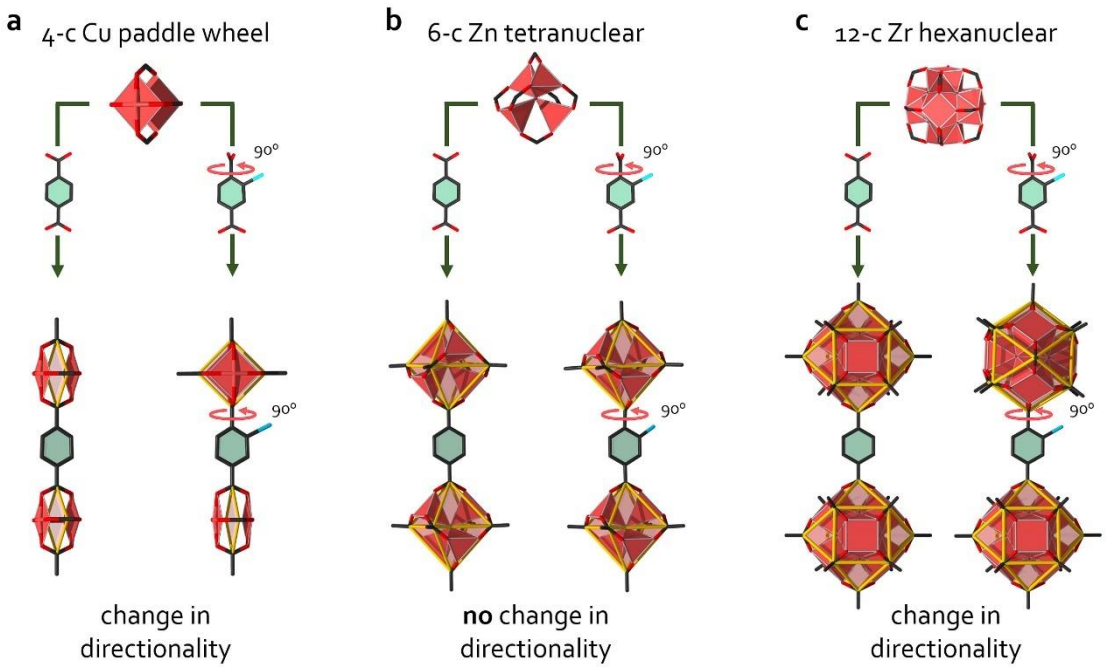

Figure 4. Comparison of the ideal orientation and directionality of MBBs with coplanar or 90º-twisted dicarboxylate ligands. Upon a 90º twist, Cu paddle wheels (a) and Zr hexamers (c) undergo a change in directionality, whereas Zn tetramer (b) maintain their directionality.

4. Bent ligands: the door to polymorphism

*In this section, the default topologies are the edge-transitive **sql** net (4-c), in the case of 4-c paddle wheels, and **fcu** net (12-c), in the case of Zr/Hf hexanuclear clusters ("UiO type cluster"). Both types of MOFs assemble by bridging linear ligands with coplanar carboxylate groups. Breaking this linearity by introducing a bending angle (Figure 2c), through use of a bent ligand, creates geometry mismatch; consequently, the ligands that surround the same MBB end up having many distinct orientations.*

Combining paddle wheels with bent ligands of various angles leads mainly to metal-organic polyhedra (MOPs)[73, 74] and to 2D MOFs (**sql** and **kgm**).[37] For MOPs generated with square building units (paddle wheels or single metal ion), the influence of the bend-angle in the ligand is clear, enabling isolation of MOPs of various geometries and distinct organic/inorganic content (*i.e.* metal/ligand [M/L] content), which has already been well documented elsewhere.[4, 75-80] To illustrate the influence of bent ligands on MOF assembly, we have chosen hexanuclear Zr/Hf clusters as the representative inorganic MBB (Figure 5), owing to their usually high and adaptable connectivity

(from 4 to 12). Introducing an angle into a dicarboxylic ligand (*i.e.* changing the directionality of its connectivity) can, depending on the bending angle, prevent the formation of the ubiquitous **fcu**-type framework (Figure 2c). Interestingly, at an angle of 160º, such as that in the ligand 9-fluoreneone-2,7dicarboxylate (fldc), found in DUT-122, the topology remains **fcu** (Figure 5a). However, to offset the effects of the bend-angle, the clusters exhibit an overall inclination of *ca.* 14º from their ideal orientation.[81] At smaller angles, such as *ca.* 150º, as in the case of the ligands dithienothiophene dicarboxylate (dttdc) and 4,4'-(2 H-1,2,4-triazole-3,5-diyl) dibenzoate (tadiba), the angle has a large influence on the outcome, leading to the **reo**-MOFs DUT-51[82] and JLU-MOF58,[83] respectively. Interestingly, using a shorter ligand of comparable angle, 2,5-thiophenedicarboxylate (tdc), leads to four distinct structures: three 8-c nets (the **reo**-MOF DUT-67[84] [Figure 5b] and its two polymorphs, the **bon**-MOF DUT-68 [Figure 5c][84] and the **hbr**-MOF DUT-126 [Figure 5e][85]), and one 10-c net (the **bct**-MOF DUT-69 [Figure 5d][84]), whose rare topology is also found in MOF-802, which is based on the ligand 3,5-pyrazoledicarboxylate (pzdc).[25] These examples highlight the great potential of bent ligands to promote structural diversity, by conferring the bent ligands around the Zr clusters with different orientations without necessarily altering the connectivity of the binding groups (Figure 5). An intriguing case is CAU-28 (Figure 5f),[86] which comprises two crystallographically distinct 2,5-furane dicarboxylate (fdc) ligands, one of which exhibits a 124º angle, four of them surrounding the Zr/Ce clusters and bridging them into a Kagomé lattice. The other ligands (four per cluster), which have a markedly smaller angle (*ca.* 103º), act as "pillars" between the layers along the *z* axis, to form an overall **kag** topology.

No section on bend-angles would be complete without mentioning a bent ligand with a 120º angle. Surprisingly, and to the best of our knowledge, no one has yet reported assembly of a MOF from Zr clusters and the ubiquitous 120º bent isophthalate ligand (*m*-bdc). However, Xie *et al.* did recently report combination of Zr clusters with either 4,4'-(benzene-1,3-diyl)dibenzoate (bdb) or 4,4'-(naphthalene-2,7-diyl)dibenzoate (ndb) to form the **pcu**-MOFs BUT-66 (Figure 5g) or BUT-67, respectively.[87] Although their clusters are 12-connected, these MOFs exhibit the same topology as in MOF-5: each Zr cluster is bridged to six others by pairs of ligands. Similarly to Xie *et al.*, Wei *et al.* subsequently reported that combination of Gd hexanuclear clusters and tetrafluoroisophthalate (*m*-bdc-F_4) generates a **pcu**-MOF.[88]

Finally, Krause *et al.* evaluated an even smaller angle, of 90º, in their assembly of a MOF from Zr clusters and the ligand 9h-carbazole-3,6-dicarboxylate (cdc) into the 1D coordination polymer DUT-80 (Figure 5h). In this

structure, the 8-c Zr clusters are quadruple-bridged to each other by cdc ligands to form "chains" of clusters, which can be connected together to yield the flexible MOF DUT-98 (*vide infra*).[89]

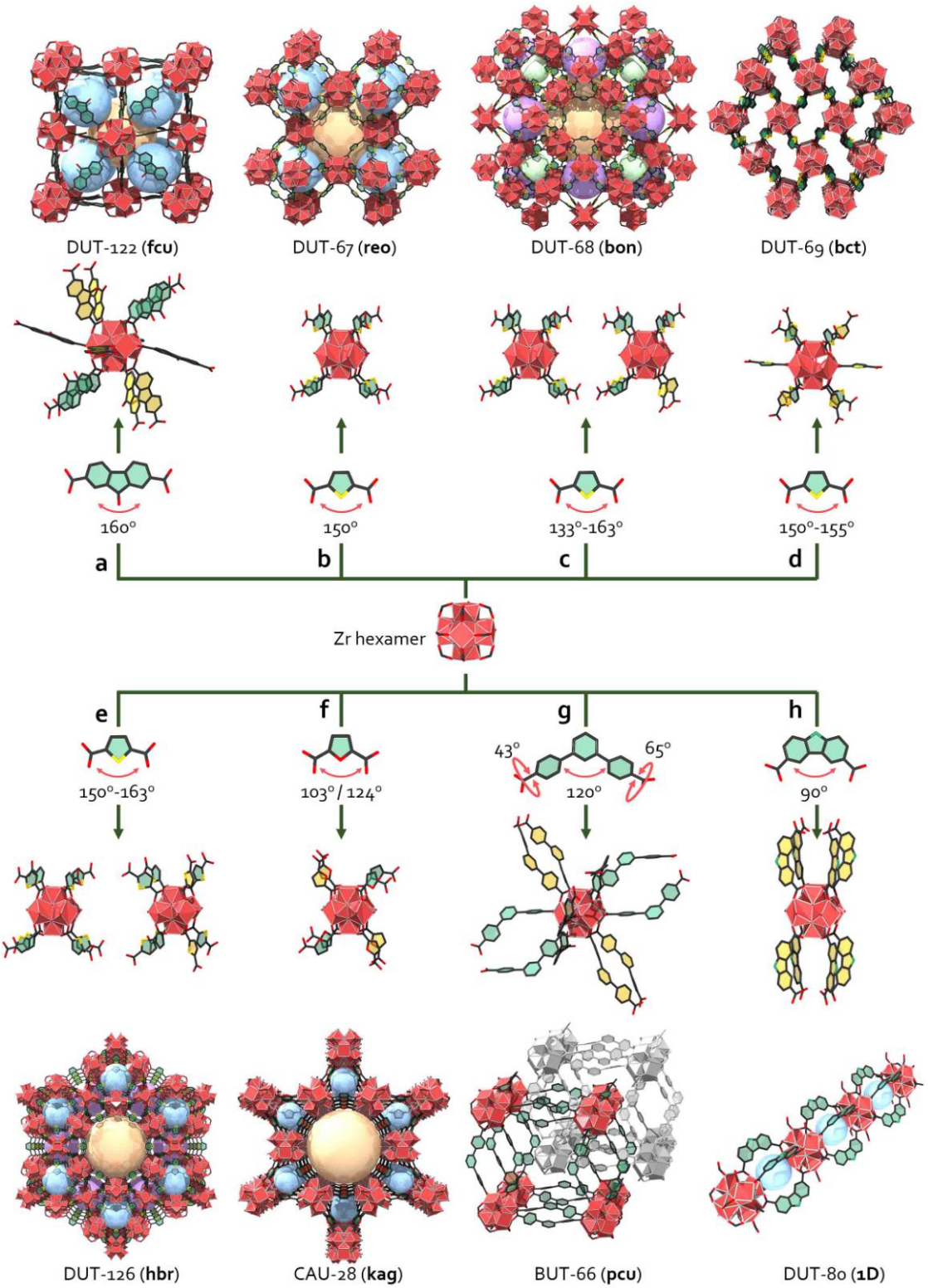

Figure 5. Varying the angle, and/or the orientation around Zr based clusters, of bent ligands leads to MOFs with a) the **fcu** (DUT-122), b) **reo** (DUT-67), c) **bon** (DUT-68), d) **bct** (DUT-69), e) **hbr** (DUT-126), f) **kag** (CAU-28) or g) **pcu** (BUT-66) topologies, as well as to 1D coordination polymers (DUT-80). Some organic rings are filled in yellow to better distinguish the ligand orientations around the clusters.

5. Zigzag ligands: transversal reticular chemistry

*In this section, the default topology is the edge-transitive **fcu** net (12-c) with Zr/Hf hexanuclear clusters ("UiO type cluster"). Such MOFs assemble by bridging linear ligands with coplanar carboxylate groups. Breaking this linearity by introducing a transversal offset creates geometry mismatch (Figure 2d).*

In addition to linear, twisted or bent ligands, another type of ditopic bridge, *zigzag ligands* (Figure 2d), is currently gaining attention in MOF assembly.[90] Examples of MOFs built with such ligands, in which the collinearity between chelating groups is broken, have been reported.[91-93] However, before the advent of transversal reticular chemistry, no clear focus had been made on the potential of their unique shape (Figure 6a).[50] By adding the transversal parameter of width (**w**) to the height (**h**) of the ligands, Guillerm *et al.* demonstrated that, along with making ligands taller or shorter, they could also stretch them transversally, thus breaking the collinearity of the binding carboxylates. In the case of Zr-based MOFs, this effect is reflected by generation of geometry mismatch (Figure 6b), as zigzag ligands do not match the perfect alignment of Zr clusters. Thus, assembling Zr clusters with zigzag ligands leads to **bcu**-MOFs, which can be regarded as **fcu**-MOFs with systematic, ordered defects — namely, four missing ligands on each MBB (Figure 6c).[50] Guillerm *et al.* reported Zr-**bcu**-MOFs (Figure 6e-h) with *trans, trans* muconate (tmuc), 2,6-naphthalene dicarboxylate (26ndc), 2,2'-bipyridine-4 4'-dicarboxylate (22bipy44dc) or azobenzene-3 3'-dicarboxylate (azo33).[50] Additionally, Maurin, Serre and co-workers used simulations to predict that Zr clusters and zigzag succinate (suc) ligand would combine to form another MOF, Zr-**bcu**-suc (MIP-204, Figure 6d), whose assembly they subsequently confirmed experimentally.[94]

Shortly after, by introducing steric hindrance by the mean of a sulfonic group on a 26ndc ligand, Nguyen *et al.* showed the possibility to not only deviate from the 12-c **fcu** net to the 8-c **bcu** net, but also to assemble its polymorphic analog, the 8-c **reo** net.[95]

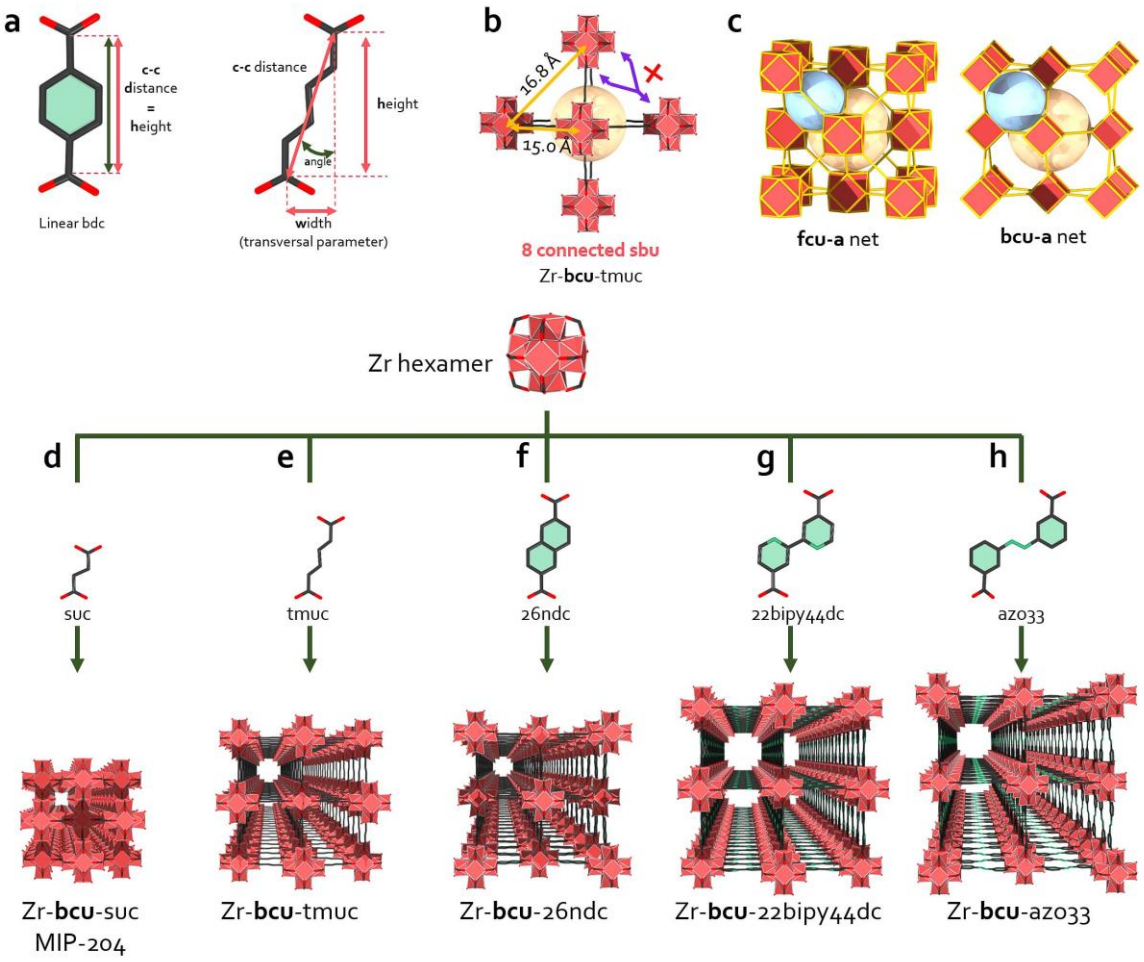

Figure 6. a) Comparison of the characteristic distances and angle in bdc (linear) and tmuc (zigzag) ligands. b) schematic of the geometry mismatch in Zr-**bcu**-tmuc. c) comparison between the **fcu-a** and **bcu-a** nets. A family of isoreticular Zr-**bcu**-MOFs based on d) suc, e) tmuc, f) 26ndc, g) 22bipy44dc or h) azo33 ligands.

The case of ligands with small widths, such as 26ndc and azobenzene-4 4'-dicarboxylate (azo44), is worth mentioning. Some of these act as linear ligands, as their disorder in the framework compensates for their small width values without affecting the cluster orientation or reducing the overall symmetry (Figure 7).[84, 96]

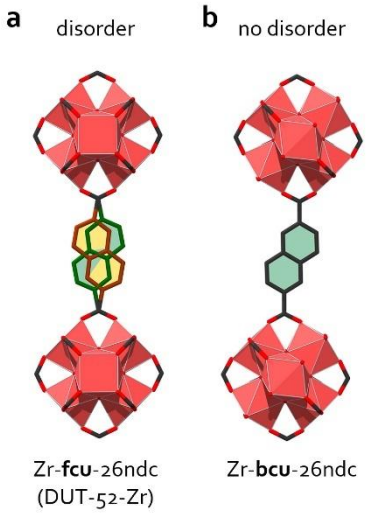

Figure 7. Detail of the 26ndc ligand disordered in Zr-**fcu**-26ndc (DUT-52-Zr) and ordered Zr-**bcu**-26ndc

Multi-functionality has recently become a highly-desired property for MOFs, as it facilitates their selective post-synthetic modification.[97, 98] Many multivariate MOFs have been reported,[9, 99-105] most of which contain randomly distributed ligands having similar shapes but carrying diverse functional groups.[103] Strategies to achieve ordered multi-functionality include ligand insertion/pore partition,[65, 66, 106] use of programmed pores[107] and assembly of merged nets[9]. Transversal reticular chemistry is taking crystal engineering to the next level, by enabling selective postsynthetic placement of ligands (*i.e.* functional groups) to create materials that mimic natural structures such as proteins and nucleic acids. For instance, Kim *et al.* reported ready functionalization of the MOF Zr-**bcu**-26ndc (Figure 8a) with tagged terephthalates to produce ordered, multivariate **fcu**-MOFs.[108] To complete the coordination of the Zr clusters in Zr-**bcu**-26ndc assembled through transversal reticular chemistry (*vide supra*), they filled the resultant unoccupied positions with their desired ligand (Figure 8b).

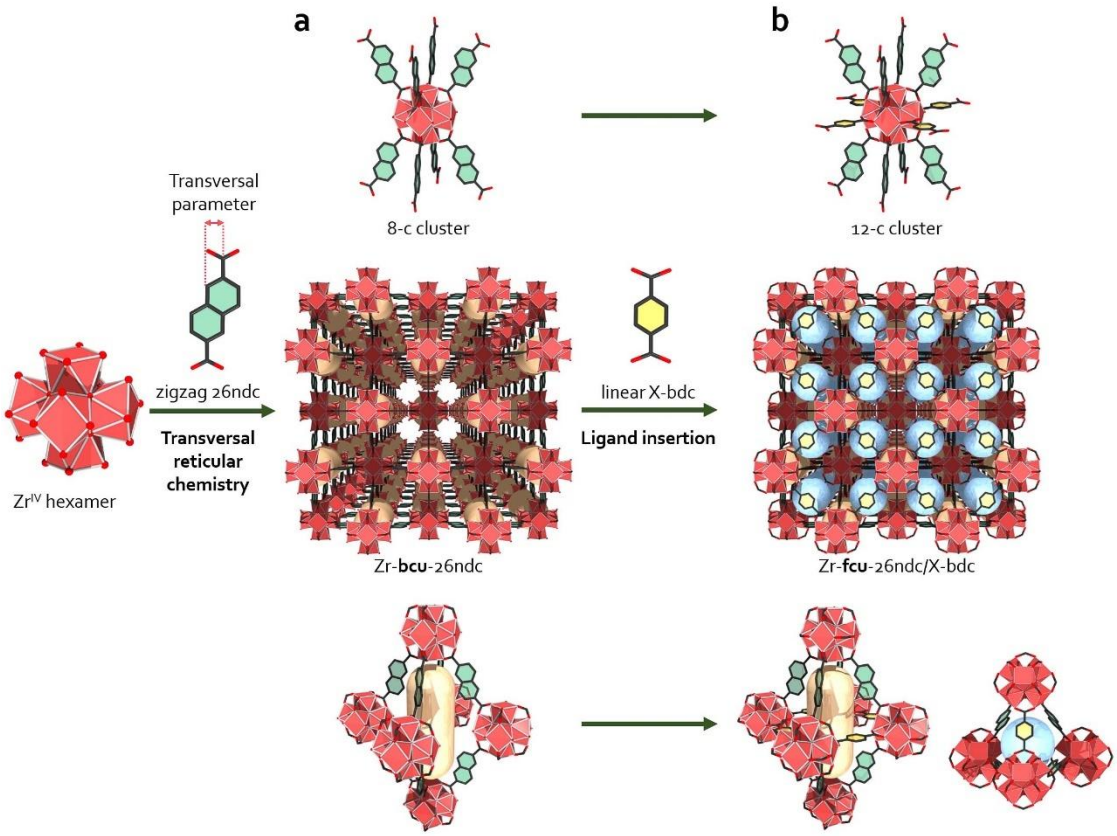

Figure 8. Transversal reticular chemistry enables precise insertion of additional ligands to transform a) Zr-**bcu**-26ndc into b) Zr-**fcu**-26ndc/bdc, by completing the coordination of the Zr hexamer (from 8-c to 12-c). Consequently, the channels in Zr-**bcu**-26ndc are transformed into the tetrahedral cages in Zr-**fcu**-26ndc/bdc.

Introducing a zigzag ligand into a MOF can influence the MOF's geometry without impacting its overall topology (Figure 9). For example, Chevreau *et al.* described the case of MIL-142B (Figure 9a), an Fe-**nht**-MOF constructed with 4,4'-biphenyldicarboxylate (44bpdc) and 4,4',4'',-benzene-1,3,5-triyl-trisbenzoate (btb),[99] whose framework is interpenetrated, yet whose transversal reticular analog, MOF-909 (Figure 9b), which contains azo33 instead of 44bpdc, comprises a single **nht** net. This is due to the distortion of the framework, preventing intergrowth of a second **nht** net.[109] Interestingly, Nguyen *et al.* reported that introduction of 50% of azo33 is sufficient to prevent its interpenetration (MOF-908).

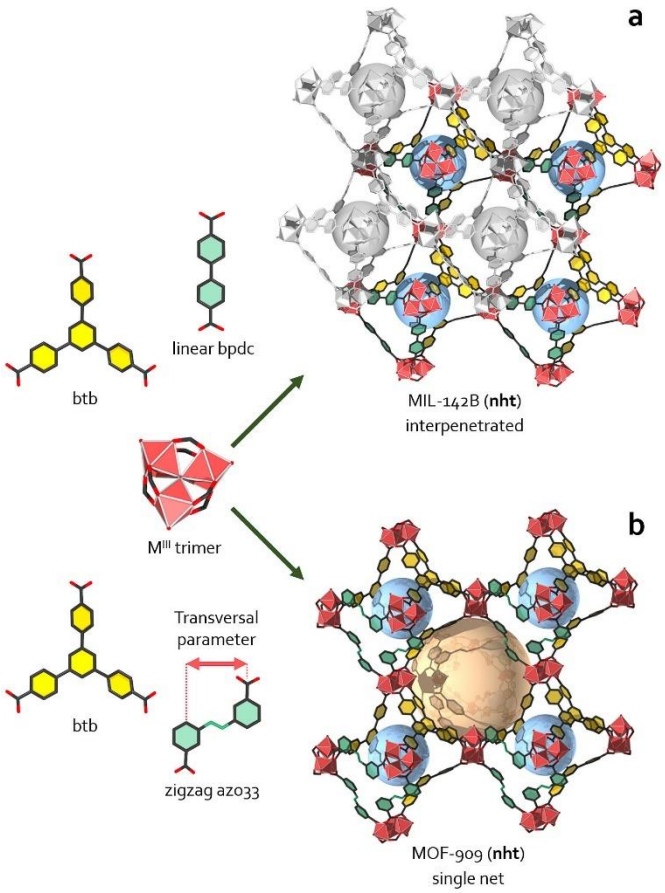

Figure 9. a) In **nht**-MOF MIL-142B, substituting linear 44bpdc with b) zigzag azo33 in MOF-909 prevents interpenetration.

6. Polytopic ligands with various angles and/or twists

6.1. Triangular ligands and cuboctahedral building blocks: geometry mismatch *par excellence*

In this section, there is no edge-transitive net to assemble regular triangles (equilateral, coplanar carboxylates) with 12-c Zr/Hf/RE hexanuclear clusters ("UiO type cluster"). Therefore, all existing structures arise from geometry mismatch, which explains the high variety of topologies (Figure 10).

6.1.1. The rare earths example. In 2014, upon noticing the apparent incompatibility of 3-c ligands with 12-c (cuboctahedra) clusters (which lacks a corresponding edge-transitive net), Guillerm *et al.* envisioned the possibility of unveiling novel clusters and topologies, which had yet to be discovered in rare-earth and MOF chemistries.[32] After determining the conditions to form the desired rare-earth hexanuclear cluster as a discrete entity, they used similar conditions, in combination with btb. Their system was highly versatile, as additional metal ions and

carboxylates caused the hexanuclear cluster to spontaneously evolve into an 18-c, nonanuclear cluster, which was compatible with 3-c btb and gave rise to an unprecedented, minimal transitive, (3,18)-c net with **gea** topology (Figure 10a). Further studies on this net revealed its suitability for rational design of MOFs using supermolecular building blocks (SBBs),[4] which we discuss later in this review.[32] Subsequently, Eddaoudi and co-workers also studied the effects of varying the angles of 3-c ligands.[34] Using the 90° angle provided by the ligand 9-(4-carboxyphenyl)-9H-carbazole-3,6-dicarboxylate (bcdc), they were able to unveil yet another nonanuclear cluster, a 12-c one that differs slightly from that observed in **gea**-MOF-1 (Figure 10a) and which led to formation of a MOF with a novel (3,12,12)-c net, **aea** topology (Figure 10b). In parallel, they demonstrated that reducing two branches of the btb ligands (*e.g.* by using the [1,1'-biphenyl]-3,4',5-tricarboxylate ligand [bptc]) generated another previously unknown topology, **pek**, and that in the resulting **pek**-MOFs (Figure 10c), a 12-c nonanuclear cluster coexisted with the classical hexanuclear cluster (albeit, with connectivity reduced to eight). Finally, by using the extended ligand 5-(4-carboxybenzyloxy)isophthalate (obi), they prepared the isoreticular analog **pek**-MOF-2. Inspired by these reports, Wang *et al.* recently discovered three novel MOFs in the RE/3-c ligand system: PCN-912 (Figure 10d), PCN-918 (Figure 10e) and PCN-909 (Figure 10f). They obtained these MOFs by reducing one branch of the btb ligand and introducing various levels of steric hindrance (using functionalized [1,1':3',1"-terphenyl]-4,4",5'-tricarboxylate ligands [R-tptc]).[43] They unveiled two novel highly-connected nets: the (3,3,12)-c net, **flg** (PCN-912); the (3,3,18)-c net, **ytw** (PCN-918); and also isolated a **sep**-MOF (PCN-909), with the same (3,9)-c net as in the previously reported Zr based MOF, BUT-39 (*vide infra*).[110]

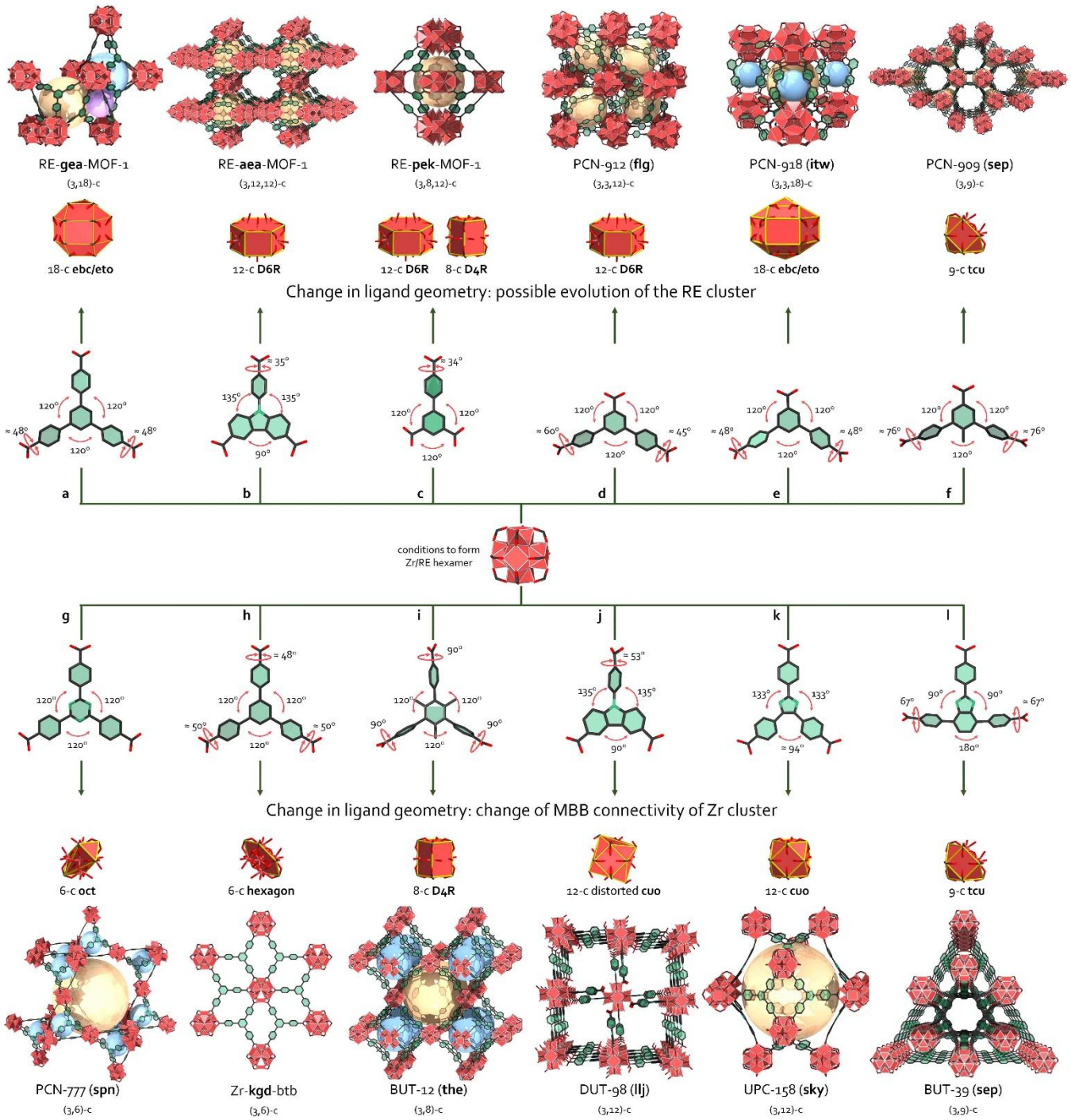

Figure 10. a-f) Summary of the RE-based MOFs and g-l) Zr-based MOFs resulting from assembly of RE/Zr with triangular ligands in the appropriate conditions to form RE/Zr hexanuclear clusters.

6.1.2. The zirconium example. Under many synthetic conditions, zirconium can produce a similar hexanuclear cluster to that of rare earths (*vide supra*).[111, 112] Since the first report of UiO-66 in 2008,[53] and given the success

achieved by forcing competition between monotopic acids (as modulators) and polytopic acids in their crystallization,[40, 70, 71, 113] Zr-MOFs have become some of the best-studied MOFs.[33, 114-116] These findings paved the way towards construction of MOFs with topologies other than **fcu**. For instance, in 2012, Morris *et al.* described assembly of Zr-MOFs with square ligands. They obtained the expected MOF-525 and MOF-535, which exhibit the edge-transitive **ftw** topology, and surprisingly, also obtained MOF-545, which shows another edge-transitive net, **csq**, whose hexanuclear cluster exhibits a connectivity reduced to eight (the first-ever reported example of this in a MOF).[58]

Regarding equilateral triangular ligands with coplanar carboxylate groups, since they cannot be assembled with 12-connected cuboctahedral shapes, the clusters instead reduce their connectivity to eight, to fit to edge-transitive nets having lower connectivity. This adaptability of the Zr clusters explains the generation of the two **spn**-MOFs MOF-808[25] (ligand: trimesate [btc]) and PCN-777 (ligand: 4,4′,4″-s-Triazine-2,4,6-triyl-tribenzoate [tatb], Figure 10g),[117] whose Zr clusters are six-connected with octahedral directionality. Similarly, Wang *et al.* reported that in presence of btb, Zr clusters also exhibit six-connectivity, albeit in hexagonal directionality, leading to formation of a **kgd**-MOF based on edge-transitive **kgd** layers that interpenetrate to form an overall 3D framework (Figure 10h). In this MOF, the carboxylates are slightly twisted (38º and 46º) relative to the ligand plane.[118] An example of a MOF in which the carboxylates show a greater twist angle (90º) was given by Wang and co-workers, who reported that Zr clusters reacted with 4,4',4''-(2,4,6-trimethyl-benzene-1,3,5-triyl)tribenzoate (Me_3btb) adopt a connectivity of eight, with cubic directionality, to yield BUT-12 (Figure 10i), a MOF with the edge-transitive **the** topology.[119] Likewise, the use of other ligands sharing the geometry of Me_3btb, 6,6′,6″-(2,4,6-trimethylbenzene-1,3,5-triyl)tris(2-naphthoate)) (tnna) or 4,4',4''-[benzene-1,3,5-triyl-tris(benzene-4,1-diyl)]tribenzoate (bbc), leads to two other **the**-MOFs: BUT-13[119] and MOF-1005, respectively.[120] Despite the adaptability of the connectivity of the Zr clusters, which helps to form MOFs of highly regular structure and edge-transitive nets, He *et al.* found that use of the highly original T-shaped ligand 4,4′,4″-(1H-benzo[d]imidazole-2,4,7-triyl)tribenzoate (btba) led to a novel, (3,9)-c topology (**sep**) within the Zr/3-c ligand system, as illustrated in their discovery of BUT-39 (Figure 10l).[110]

As we mentioned above, DUT-80 is a unidimensional structure constructed from 8-c Zr clusters and cdc, a ligand with a bend-angle of 90º. Krause *et al.* discovered that using this 1D motif with such an angle implemented in the

bcdc ligand leads to an unprecedented (3,12)-c net: they obtained the **llj**-MOF DUT-98 (Figure 10j), which exhibits high structural flexibility.[89]

Another possibility to obtain a novel (3,12)-c net was reported by Lee *et al.* in their construction of MOF-1004, which exhibits the **sky** topology, in which the geometry of the 12-c node is cuboctahedral.[120] To generate this net, they used the wide and slightly flexible ligand 4,4',4''-[benzene-1,3,5-triyltris(ethyne-2,1-diyl)]tribenzoate (bte), in which the angles between two branches is only 94º (compared to 120º in the ideal geometry of the ligand). Interestingly, Sun and co-workers followed this prerequisite in the design of their ligand 4,4',4''-(1H-imidazole-2,4,5-triyl)tribenzoate (ittc), which they subsequently used to assemble UPC-158 (Figure 10k), an isoreticular analog with the **sky** topology.[121] Their work demonstrates that even such unexpected topologies can be rationally targeted, provided that the geometrical requirements are known.

6.2. Triangular ligands with square paddle wheel building blocks

*In this section, the default topology to assemble regular triangles (equilateral, coplanar carboxylates) with paddle wheels (4-c) is the (3,4)-c edge-transitive **tbo** net. Modifying the coplanarity of the carboxylates, the angles or using ligands with unequal edge-lengths creates geometry mismatch (Figure 11).*

Although the structural and topological variety of MOFs based on paddle wheels and triangular ligands is not as rich as that for hexanuclear clusters and these ligands (*vide supra*), we do consider some examples worthy of discussing here. Combination of a regular planar ligand such as trimesate (btc) with paddle wheels leads to HKUST-1, which exhibits the **tbo** topology;[1] however, obtaining extended reticular analogs is not trivial. Interestingly, using 4,4',4''-benzene-1,3,5-triyl-tris(benzoate) (btb) instead of btc leads to two MOFs that exhibit the **pto** topology, another edge-transitive net: MOF-14[64] (interwoven) and MOF-143[122] (single net, Figure 11b). This is due to the natural twist of the carboxylates in btb. Alternatively, using a fully planar and regular ligand such as 4,4',4''-s-triazine-2,4,6-triyl-tribenzoate (tatb) or 4,4',4''-(benzene-1,3,5-triyl-tris)benzene-4,1-diyltrisbenzoate (bbc), affords the expected **tbo**-MOFs PCN-6 (Figure 11a)[123] or MOF-399,[122] respectively.

Another approach to access unusual topologies from paddle wheels and triangular ligands is simply to elongate one or more ligand branches. For instance, Wong-Foy *et al.* employed biphenyl-3,4,5-tricarboxylate (bptc) to elongate one branch of btc, enabling them to assemble UMCM-150 (Figure 11c), a MOF resulting from the pillaring of

Kagomé layers (**kgl**) by a rare Cu trimer to generate the **agw** topology. The layers are constructed from paddle wheels bridged by the isophthalic moieties of the bptc ligands, whereas the remaining benzoic moieties alternately point up or down from the layers, such that another paddle wheel cannot be incorporated, thus "forcing" formation of a 6-c Cu trimer.[124] Lim *et al.* reported that this Cu trimer could be substituted with other metal trimers (Co, Fe, Ni),[125] and Lu *et al.* found that the ligand could be further extended to obtain greater porosity.[126] Similarly, Schnobrich *et al.* used terphenyl tricarboxylate (tptc) to elongate two branches of the btc ligand, ultimately obtaining a UMCM-151 structure that contains paddle wheels only, albeit in an unpredictable, complex, pentanodal (3,3,4,4,4)-c net, **fmj** topology (Figure 11d).[127]

In addition to varying the carboxylate orientation and/or elongating the ligand branches, another approach to obtain dramatically different topologies is to introduce a 90º angle between two branches of the ligand by using carbazole groups, such as those in 4,4′-(9-(4′-carboxy-[1,1′-biphenyl]-4-yl)-9H-carbazole-3,6-diyl)dibenzoate (bpcdc). For example, Stoek and co-workers rationally designed DUT-75 (Figure 11e) and DUT-76 (**gee** topology) by using the SBB approach to adopt overall **ftw**-type structures.[128] Exploiting the possibility to form carbazole-based MOPs with cuboctahedral shapes,[129] they simply linked the 12-extremities together through a paddle wheel.

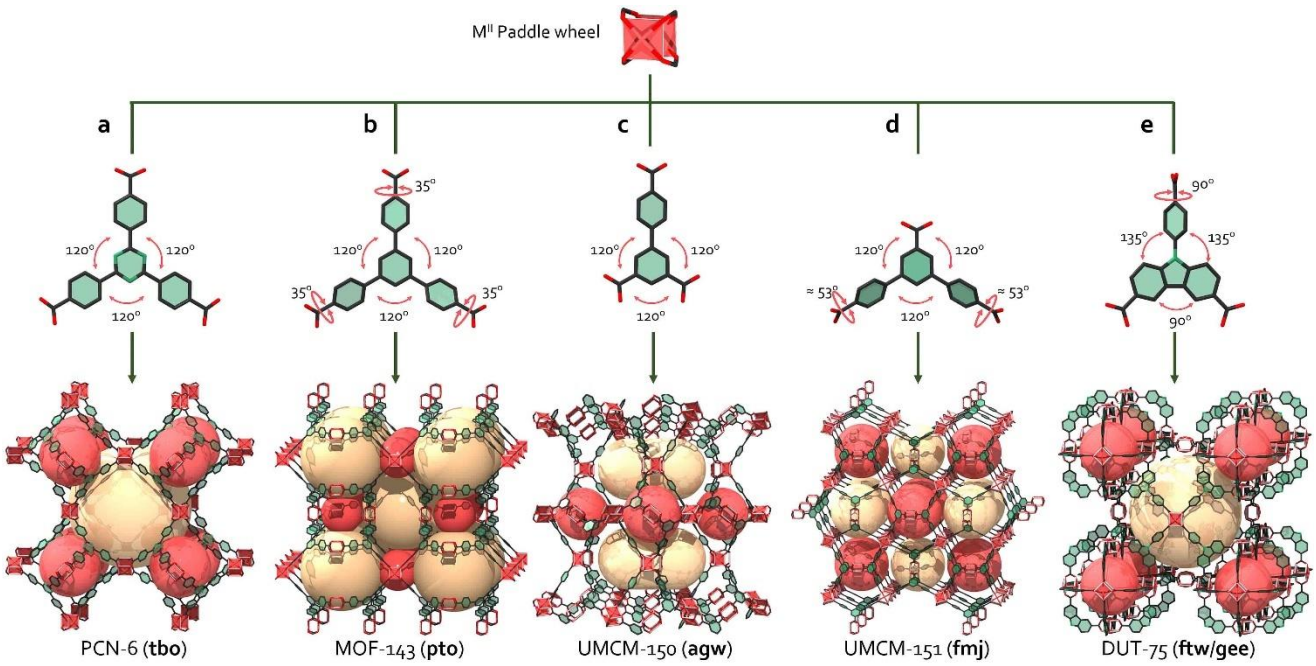

Figure 11. Summary of the Cu-based MOFs resulting from assembly of paddle wheels with triangular ligands. The geometric differences among 3-c ligands strongly influence the resulting MOF structures, leading to the a) **tbo** (PCN-6), b) **pto** (MOF-143), c) **fmj** (UMCM-150), d) **agw** (UMCM-151) or e) **ftw**/**gee** (DUT-75) topologies.

6.3. Triangular ligands with 6-c trigonal prismatic building blocks

*In this section, there is no edge-transitive net with which to assemble regular triangles (equilateral, coplanar carboxylates) with 6-c M^{III} (Fe, Al, Cr, Ga, In, etc.) trimers. Given the high incidence of the **moo** net, which derives from the zeolitic **mtn** net, we can consider it to be the default net for these assemblies. Modifying the coplanarity of the carboxylates, the angles using ligands with unequal edge-lengths leads to geometry mismatch (Figure 12).*

Although assembly of regular triangular ligands with 6-c trigonal prismatic MBBs cannot generate an edge-transitive net, various compatible nets with only two types of edges have been reported, including the **ceq**, **dag**, **hwx**, **sit** and **ydq** topologies. Surprisingly, most MOFs in this system adopt the extremely complex, decanodal **moo** topology of MIL-100.[52] This assembly had first been predicted by simulations[130, 131] and can be explained by formation of super-tetrahedra that favor further self-assembly of MOFs into an overall zeolitic (**mtn** type) topology, as observed in the examples of MIL-100,[52] MIL-100-btb,[132] PCN-332,[133] PCN-333[133] and PCN-888 (Figure 12a).[134]

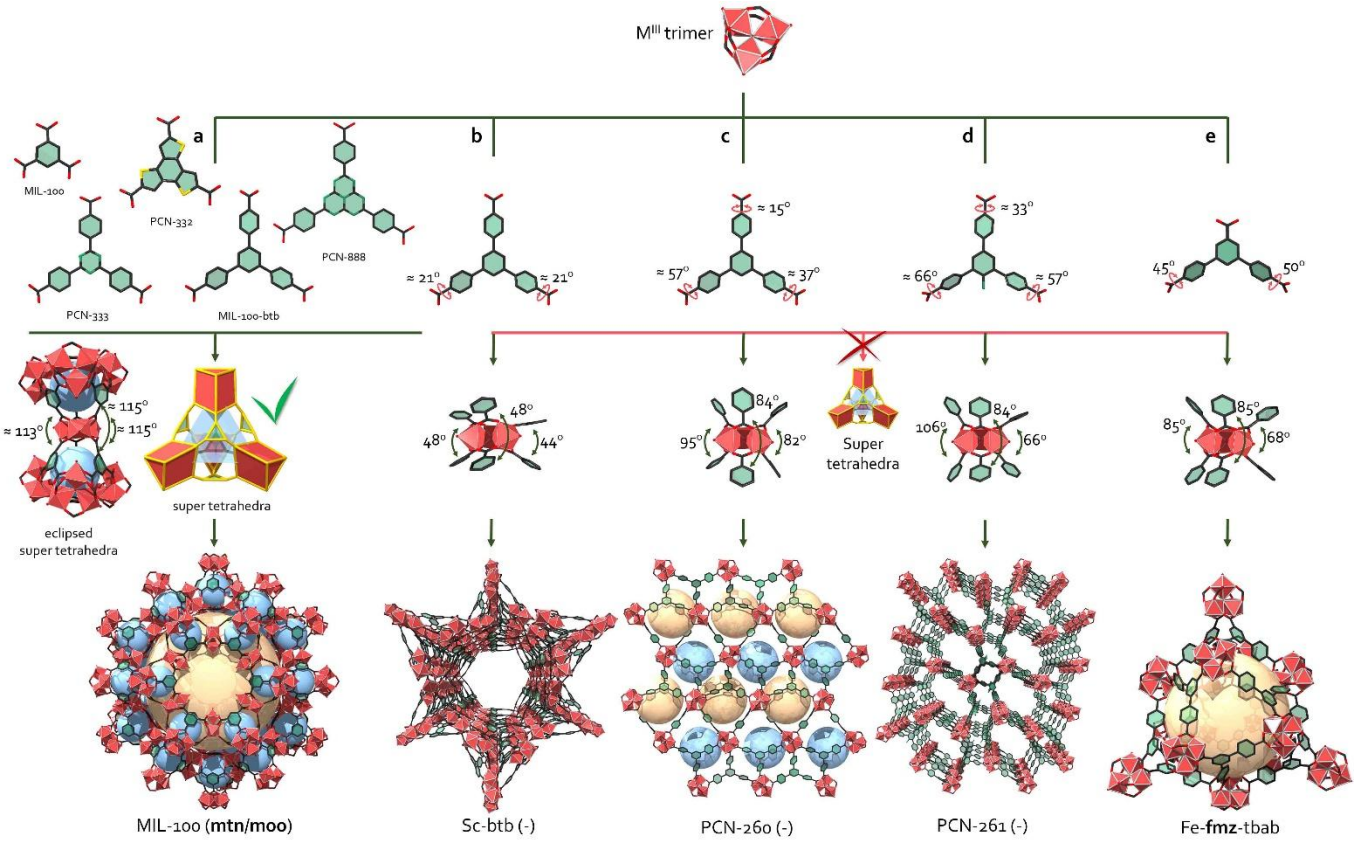

Figure 12. a) Equilateral triangle ligands with coplanar carboxylates assemble with trimers to form supertetrahedra, that further assemble into an underlying zeolitic **mtn** type network (**moo**-MOFs). Breaking the coplanarity leads to other types of MOFs, b) Sc-btb, c) PCN-260 and d) PCN-261), whereas e) using tbab yields the Fe-**fmz**-tbab structure.

Intriguingly, and similarly to other systems that we discuss in this review, not all assemblies of regular triangular ligands with 6-c trigonal prisms lead to the **moo** topology. For example, when Ibarra and co-workers assembled btb, which *can* yield **moo** MOFs,[132] with scandium trimers, they instead obtained the MOF Sc-btb (Figure 12b), which exhibits a different topology, (3,6)-c (not described in the RCSR database).[135] This is not surprising, given that the carboxylates from btb are naturally out of plane, as has been observed in other systems.[32, 64, 118, 136] Additional examples of MOFs constructed from btb (PCN-260, Figure 12c), or amino- (PCN-261, Figure 12d) or hydroxyl- (PCN-261) functionalized btb, also derive from the **moo** net. In these MOFs, geometry mismatch again resides in the *natural twist* (3,3,3,6,6)-c net, **xxx** topology; for PCN-260 or *forced twist* (3,3,6)-c net, **yyy** topology; for PCN-261 and PCN-262 of the carboxylates.[137]

Although it is difficult to know if it is a parameter governing the topology, or resulting from it, the angles formed by the ligands around the clusters vary significantly from one structure to another, and are far from the *ca.* 115° angle required to form the supertetrahedra necessary for the assembly of **mtn**/**moo** type MOFs (Figure 12).

Another example of geometry mismatch in these systems is to replace btb with a ligand that has one shorter branch (*e.g.* tbab), such that upon assembly of the ligand with the metal trimer, the shorter branch length precludes formation of super-tetrahedra. In this sense, the assembly of tbab with Fe, Ga, In or Al trimers to yield Fe-MOF (Fe-**fmz**-tbab, Figure 12e) and SNNU-5, which exhibit a (3,6)-c net, **fmz** topology.[138, 139]

6.4. Triangular ligands with 6-c octahedral building blocks

*In this section, **pyr** is the edge-transitive net to assemble regular triangles with 6-c Zn tetramers ("MOF-5 type" cluster). They require equilateral ligands with highly twisted carboxylate groups of the ligand (*i.e. *relatively flexible branches). Non-equilateral ligands, ligands with lower coplanarity and ligands with less-twisted carboxylates all generate geometry mismatch (Figure 13).*

There are several examples of regular triangular ligands being assembled with 6-c octahedral Zn tetramers to form **pyr**-MOFs, including MOF-150, constructed with 4,4',4''-tricarboxylate triphenylamine (tca) (Figure 13a);[140] MOF-155-J, built with 1-(3-amino-4-carboxyphenyl)-3-(4-carboxyphenyl)-5-(4-carboxynaphthalen-1-yl)-benzene (btb-*m*NH_2);[141] and MOF-950, made from benzene-1,3,5-tri-β-acryate (btac).[142] However, MOF-177 (Figure 13b),[136] built from btb, and its many (> 20) functionalized[141] or extended analogs,[143] are all based on the "queen of MOFs", the **qom** net. In these cases, preferential generation of **qom** over **pyr** is due to the weaker twisting of the carboxylates in the ligands used in the **qom** MOFs. However, contrary to a common assumption[136] – and as we explained in the previous paragraph – the carboxylates in the constituent btb ligands of MOF-177 are not coplanar. Another MOF based on different carboxylate twists induced by the use of btb ligand with steric hindrance is MOF-156-J, which exhibits the **rtl** topology (Figure 13c).[141]

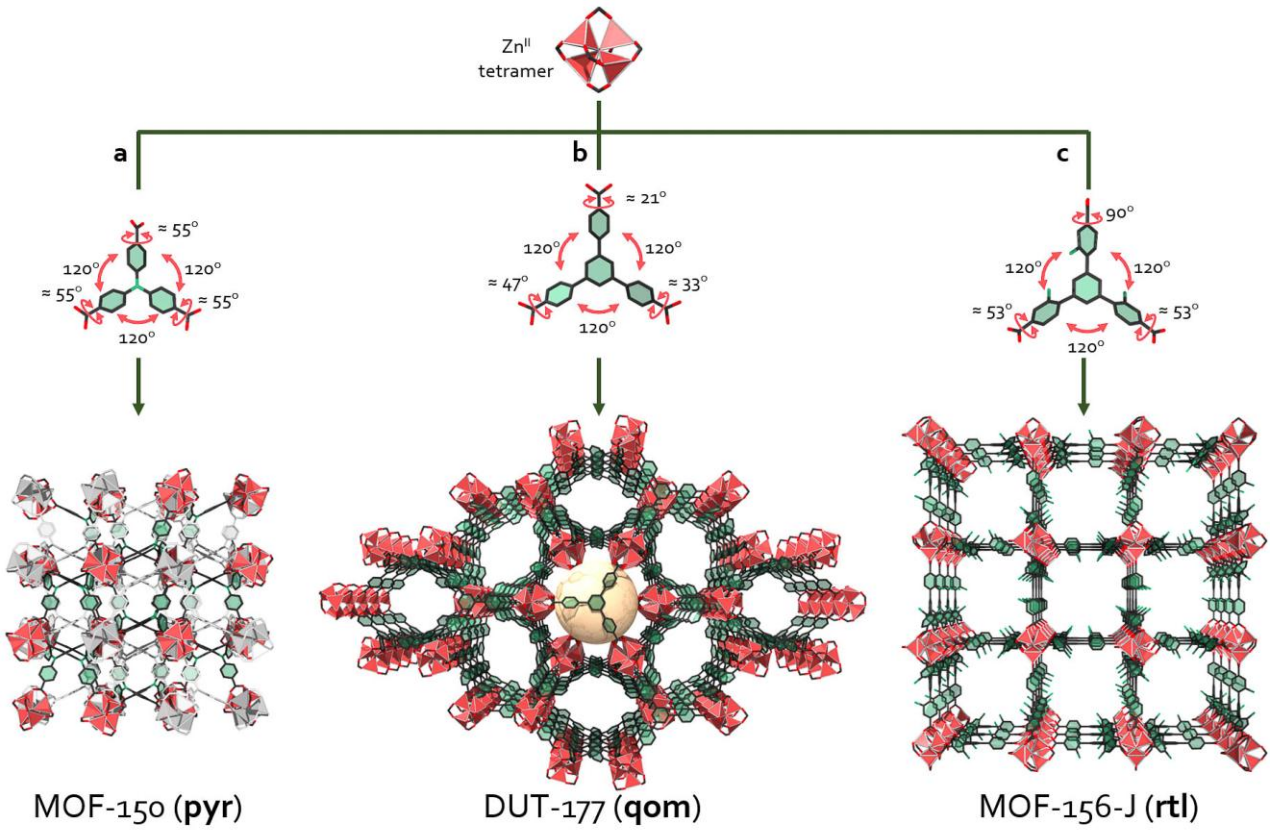

Figure 13. Combining zinc tetramers with triangular ligands that differ by carboxylate-twisting can yield to a) **pyr** (MOF-150), b) **qom** (MOF-177) or c) **rtl** MOFs (MOF-156-J).

In addition to modifying the level of twisting in the ligand carboxylates, other methods to confer systems with geometry mismatch might include altering either the ligand length[144, 145] or the angle between the ligand branches[146] (*i.e.* using non-equilateral ligands). The fact that no structure built this way has yet been reported could be explained by the idea that these approaches would likely prevent formation of the Zn tetramer; however, their possible assembly cannot be ruled out.

6.5. Square/rectangle ligands with 4-c paddle wheels building blocks

In this section, the default topology to assemble square/rectangle ligands with 4-c paddle wheels, is the (3,3,4)-c ***fof*** *net, derived from the edge-transitive* ***nbo*** *net (4-c).* ***fof*** *MOFs assemble by linking rectangle ligands with two coplanar dicarboxylate groups with a 120° angle (i.e. isophthalate). Breaking this coplanarity or modifying the dicarboxylate angle creates geometry mismatch (Figure 14).*

*Note: this section does not cover examples with ligands based on "naturally tetrahedral" ligands (*i.e. *containing sp^3 carbon, adamantane central core, etc.).*

Numerous MOFs constructed from di-isophthalic-based ligands and paddle wheels have been reported, including MOF-505 (Figure 14a),[147] and their default **nbo**/**fof** topology is widely described in the literature.[4, 148, 149] Their structures can be considered as ligand-to-ligand (L-L) pillaring of supermolecular building layers (SBLs).[4] The default SBLs are **kgl**, which are staggered in the **fof** net. Interesting non-default examples include PCN-12 (Figure 14b)[150] and ZJU-25,[151] in which bending of the central core of their respective ligands prevents staggered packing and instead, generates eclipsed pillaring to yield an **ssa**/**sty** topology. Another noteworthy example is NOTT-109 (Figure 14c),[152] in which a bulky naphthalene core precludes formation of the main cage characteristic of **nbo**/**fof** MOFs and instead, leads to formation of **sql** SBLs, which are pillared in an eclipsed fashion to form the **ssb**/**stx** topology. Researchers have built other pillared **sql** MOFs by using highly flexible ligands.[4, 153] Expectedly, such MOFs may be subject to polymorphism, depending on the ligand conformation.[154, 155] Thus, planar (rectangular) ligands lead to an overall **lvt**/**lil** topology, as in DUT-10,[153] whereas tetrahedral analogs of the same ligands (*e.g.* obtained by twisting of the dicarboxylate moieties) lead to the **pts/tfk** topology, as in DUT-11.[153]

Pillaring of SBLs is not the only way to achieve non-default topologies in MOFs assembled from di-isophthalic-based ligands and paddle wheels. As we have discussed above for other MOF families, ligand bend-angles can be chosen to dictate topology. For example, researchers have reported that in SBB assembly with paddle wheels, substituting isophthalate (120º bend) with carbazole dicarboxylate (90º bend) yields PCN-82 (Figure 14d)[156] and DUT-49 with **tfb** topology.[48, 157] In these structures, the dicarboxylate moieties combine with the paddle wheels to form cuboctahedral cages that are bridged by the central core of the ligands to generate the underlying **fcu** topology.

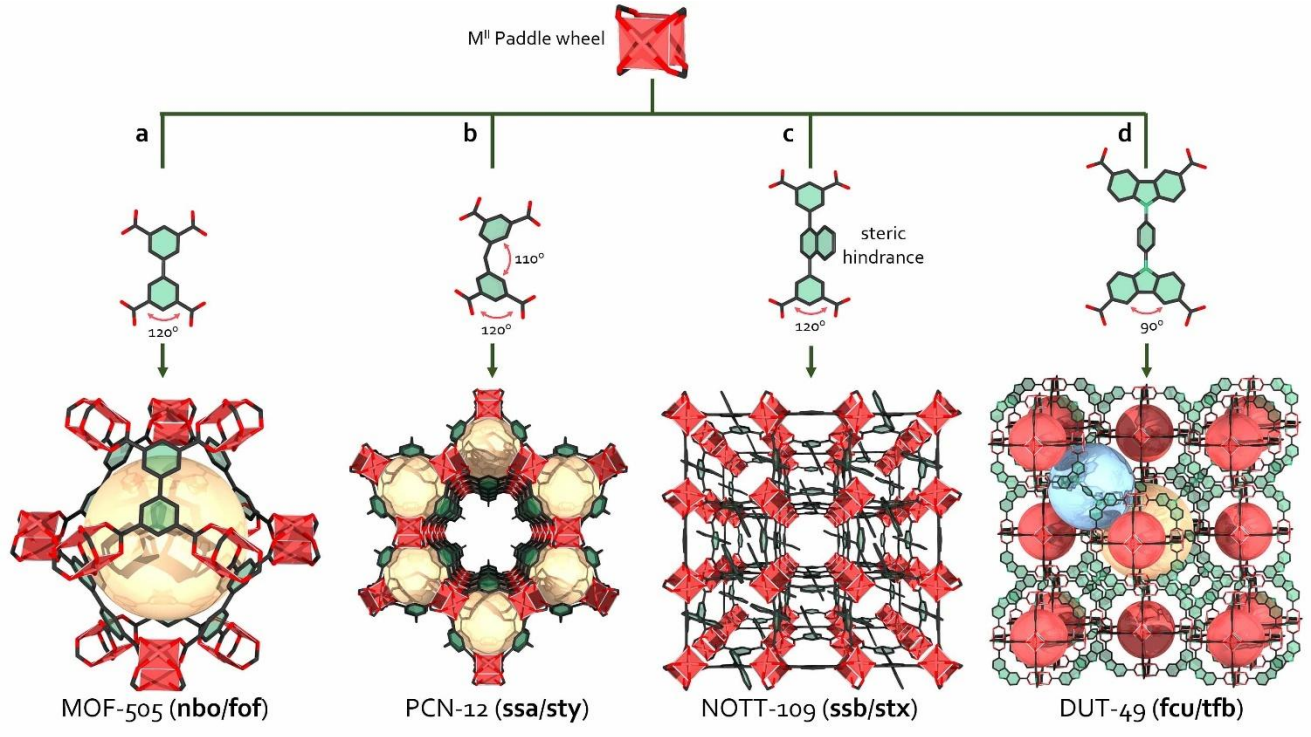

Figure 14. Assembly of paddle wheels with square/rectangular ligands mainly affords a) pillared **kgl** layers in **nbo**/**fof**-type MOFs (MOF-505). b) Introducing bending into the ligand yields a different type of pillaring, leading to the **ssa**/**sty** topology (PCN-12). c) Steric hindrance leads to pillaring **sql** into **ssb**/**stx** MOFs (NOTT-109). d) Reducing the bend-angle from 120º to 90º by replacing isophthalate moieties with carbazoles enables assembly of SBB-based **tfb**-MOF (DUT-49), whose underlying topology is **fcu**.

6.6. Square/rectangle ligands with Zr hexanuclear cluster building blocks

In this section, the default topology to assemble square/rectangle ligands with Zr/Hf/RE hexanuclear clusters ("UiO type cluster") is the edge-transitive (4,12)-c ***ftw****. MOFs assemble by linking square ligands with coplanar carboxylate groups. Breaking this coplanarity or deviating from the ideal square shape of the ligand creates geometry mismatch (Figure 15).*

*Note: this section does not cover examples with ligands based on "naturally tetrahedral" ligands (*i.e. *containing sp^3 carbon, adamantane central core, etc.).*

Beyond the expected **ftw** topology, various other edge-transitive nets have been obtained upon assembly of 4-c ligands with Zr/Hf/RE hexanuclear clusters, including **csq**,[58] **she**,[158] **scu**,[159] **shp**,[160] **flu**,[25] **ith**,[25] **sqc**,[161] **stp**[162] and

lvt.[163] This is not surprising, given the capacity of such clusters to adapt to lower connectivities (*vide supra*). Many of these topologies resulted when researchers changed the synthetic conditions or the amount of modulator previously used for **ftw** MOFs. Although Chen *et al.* described most of these in their recent review of Zr-MOFs based on edge-transitive nets,[115] we have chosen to highlight a few examples below (Figure 15).

Intriguingly, the **ftw** and **scu** nets are related. The main cage in **ftw**-MOFs can be represented as a cube, in which the clusters lying on the vertices are connected through the 4-c ligands that occupy the faces. Accordingly, elongation of the ligand in a single direction (*i.e.* by using a longer ligand) creates geometry mismatch, as only four of the six faces in the initial cage can accommodate a ligand, leaving the other two free. This scenario favors the **scu**/**tty** topology, in which 1D channels exist and the connectivity of the MBBs is reduced to eight (Figure 15). Moreover, if the length of the longer ligand is moderate compared to its width, as in the case of biphenyl-3,3′,5,5′-tetracarboxylate, bptet,[163] then an **ftw** related MOFs with **kle** topology can still be formed (Figure 15b), as first reported for RE clusters by Luebke *et al.*[164] Along these lines, Wang *et al.*, in their work on replacing the ligand bptet with the longer ligand 3,3′,5,5′-azobenzene-tetracarboxylate (azotet), obtained a rare, **scu**-derived net that is not reported in the RCSR database, in which the ligand orientation alternates and the clusters are tilted from their ideal alignment to balance the ligand length/width ratio (Figure 15c).[163] Interestingly, when they evaluated an even longer ligand, [1,1′:4′,1″]terphenyl- 3,3″,5,5″-tetracarboxylate (tptet), they obtained the first-ever Zr based **lvt/lim**-MOF, in which the connectivity of the Zr cluster is reduced to 4 (Figure 15d).

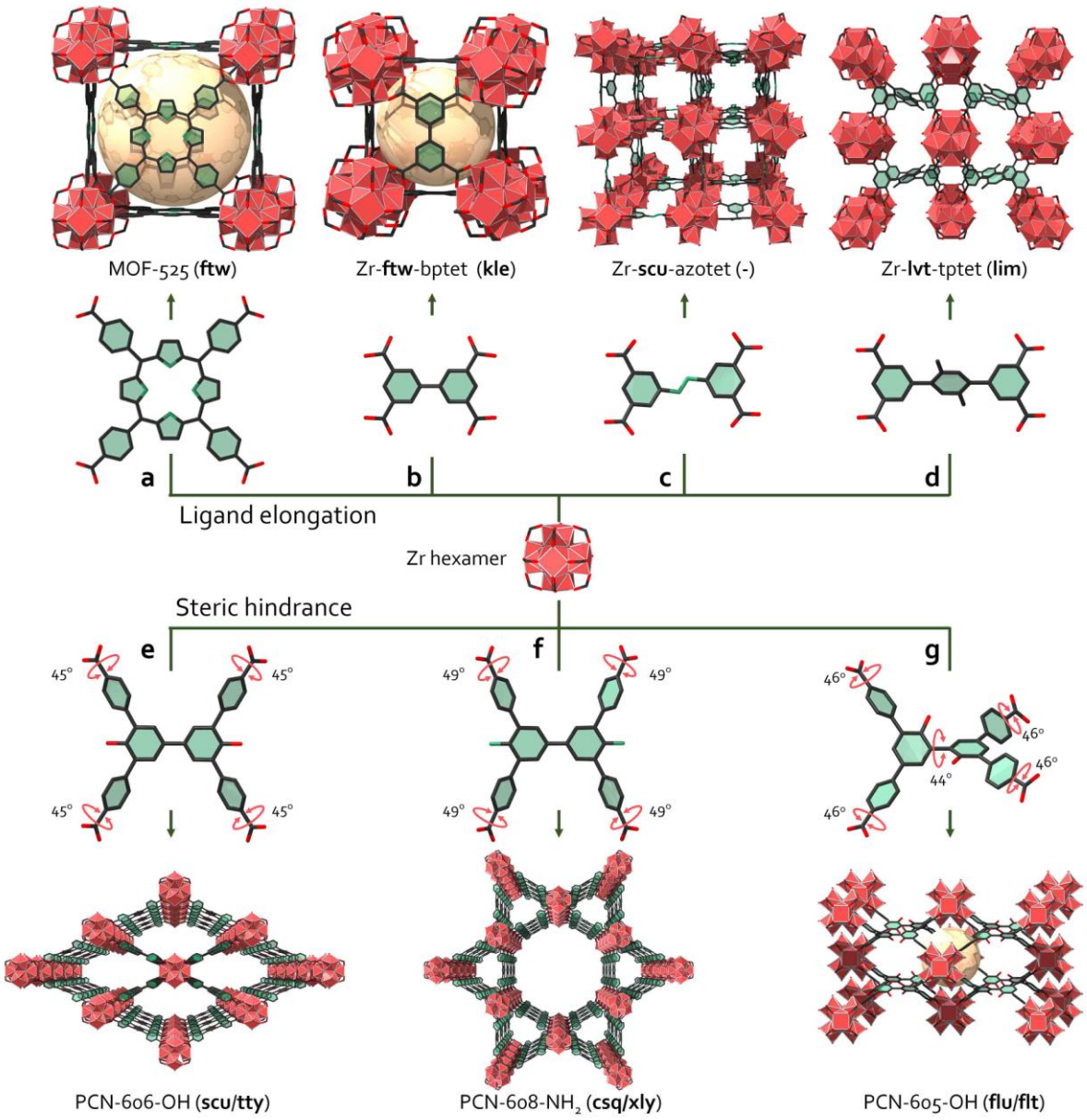

Figure 15. Although assembly of square building blocks with the ideally 12-c connected Zr hexanuclear clusters should lead to the edge-transitive **ftw** net (MOF-525), elongation of the ligand in one direction can yield **kle**, **scu/xxx** or **lvt/lim**-MOFs. By introducing steric hindrance into a rectangular ligand, the topology can be selectively controlled among **scu/tty** (PCN-606), **csq/xly** (PCN-608) or, in some cases, **flu/flt** (PCN-605).

In most cases, if a ligand's shape deviates significantly from the ideal square shape required for forming an **ftw**-MOF, then the resulting topology will be derived from **csq** (**xly** or **xlz**) or from **scu** (**tty** or **cut**). In some cases, the final geometry of the ligand, and ultimately, the resulting topology, can be controlled by introducing steric hindrance or by using ligands with a less rigid core. Indeed, Pang *et al.* reported selective control among **flu/flt**

(PCN-605, Figure 15g), **scu/tty** (PCN-606, Figure 15e) and **csq/xly** (PCN-608, Figure 15f) MOFs, via selective functionalization of a set of 4-c ligands based on 3,3',5,5'-tetra(ethyl-4-carboxyphenyl)-1,1'biphenyl (tpcb).[165] Similarly, Lyu *et al.*, were able to switch from the **scu** net in CAU-24[166] to either the **shp** net in NU-904[167] or the **csq** net in NU-1008,[167] by simply introducing one or two bulky functional groups, respectively, onto the 4,4',4",4'"-benzene-1,2,4,5-tetrayl-tetrabenzoate (tcpb) ligand. These groups directly influence the twisting of the carboxylates and therefore, dictate the resulting topology.

6.7. Hexacarboxylate ligands with 4-c square paddle wheel building blocks: not another rht-MOF

*In this section, the default topology is **ntt**, derived from the edge-transitive (3,24)-c net **rht**. Dicarboxylate bent (120^o) extremities of trefoil ligands construct externally functionalized MOPs (24-c), that act as SBBs, and are linked together by the central core of the ligand (3-c). Breaking the planarity of the ligand, or preventing the formation of a 24-c MOP by modifying the angles between carboxylates, each introduces geometry mismatch that precludes formation of **rht**/**ntt**-MOFs (Figure 16).*

In 2008, Nouar *et al.* described use of externally-functionalized MOPs as SBBs, which they assembled with copper trimers to form **rht**-MOF-1.[39] Interestingly, this trimer can be substituted with 3-connected organic cores[168, 169] to afford overall planar hexacarboxylate ligands, which have been used to assemble various **rht**-MOFs (also known as **ntt**-MOFs, Figure 16a) [39, 47, 168, 170, 171]. In parallel, Guo *et al.* reported UTSA-20 (Figure 16b), which they built with a similar type of ligand, 3,3',3'',5,5',5''-benzene-1,3,5-triyl-hexabenzoate (bhb), showing that the geometry of this ligand was too intricate and resulted in broken planarity.[172] UTSA-20 exhibits a **zyg** topology and represents one of the rare MOFs based on paddle wheels and hexacarboxylate ligands that does not exhibit the ubiquitous **rht**/**ntt** topology.

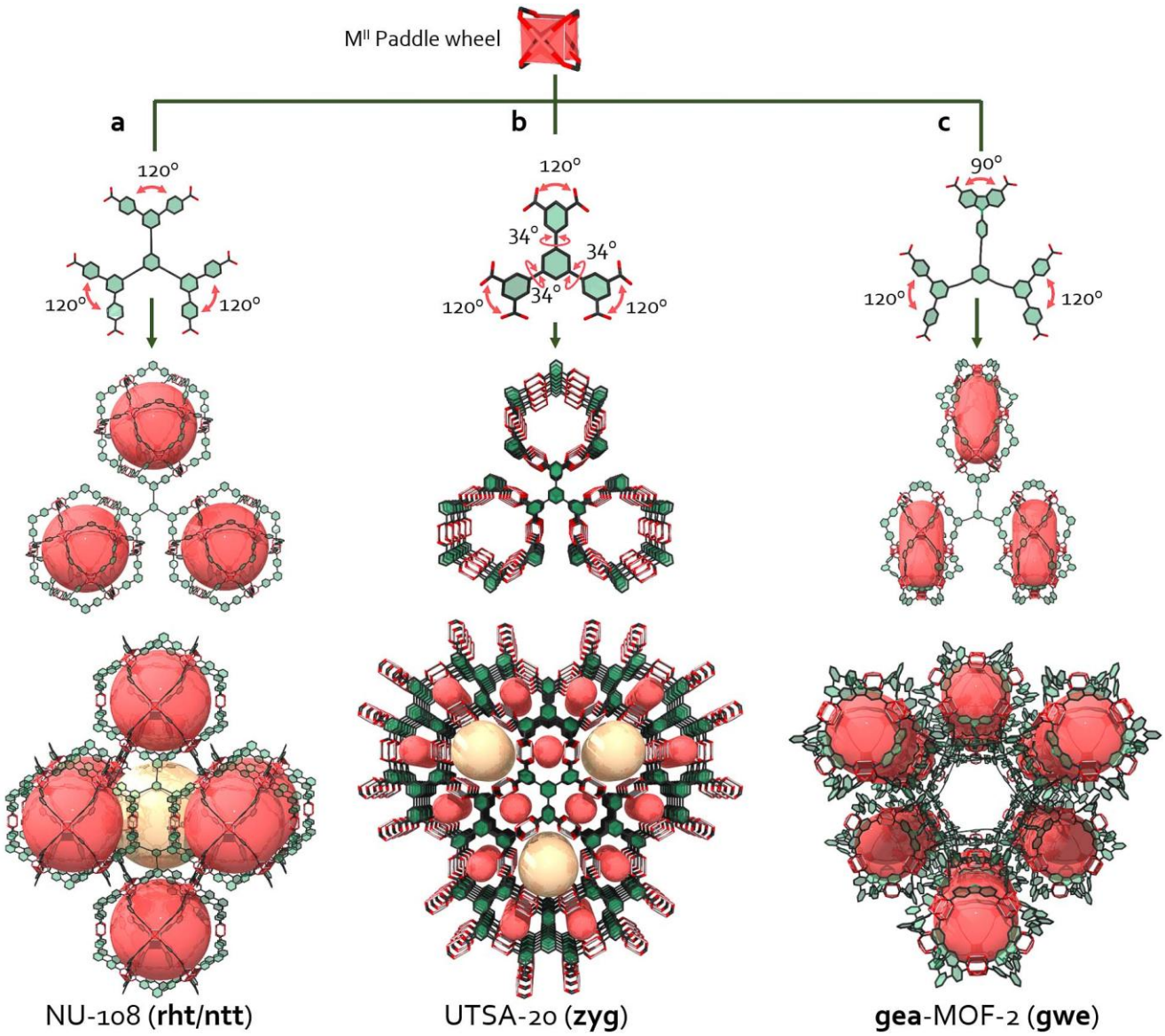

Figure 16. In addition to a) the many **rht**/**ntt**-based MOFs (NU-108) based on planar hexacarboxylate ligands, one can obtain b) **zyg**-MOF (UTSA-20), by breaking the planarity of the ligand, or c) an SBB-based **gea**/**gwe**-MOF (**gea**-MOF-2), by decreasing (from 120º to 90º) one of the angles in one of the three dicarboxylate moieties, via introduction of carbazole moieties. The latter change leads to an 18-c MOP instead of a 24-c MOP (which would be required to form **rht**/**ntt**-MOFs).

Another example of a paddle wheel hexacarboxylate MOF that does not exhibit the **rht** topology is **gea**-MOF-2 (formally: **gwe** topology), a representative case to the scope of this review, as the **gea** topology was discovered by employing a geometry mismatch strategy.[32] Indeed, **gea**-MOF-2 (Figure 16c) was rationally designed using the SBB approach, to specifically adopt an overall **gea** topology. Guillerm *et al.* identified a suitable MOP with 18

vertices[173] matching the geometry of a triangular orthobicupola (**eto**/**ebc**), corresponding to the points of extension of a newly discovered RE nonanuclear cluster with 18 points of extension in **gea**-MOF-1. By incorporating this geometric information to build the **eto**-MOP in a trefoil hexacarboxylic ligand (*i.e.* two 120º angles for one 90º angle), they were able to use the ligand 5′,5‴′-((5-((4-(3,6-dicarboxylato-9H-carbazol-9-yl)phenyl)ethynyl)-1,3-phenylene)bis(ethyne-2,1-diyl))bis((1,1′:3′,1″-terphenyl]-4,4″-dicarboxylate (lgea2) as a **net**-coded building unit[4] to replicate the underlying **gea** net, enabling its use as a blueprint for rational assembly of **gea**-MOF-2. In this sense, the 90º angle provided geometry mismatch to preclude formation of an **rht**-MOF (for which the 120º angles are crucial).

7. Conclusions

We have provided an overview of geometry mismatch-based approaches to assemble MOFs that exhibit non-default topologies, which in some cases, have enabled discovery of novel clusters that remain to be studied. These approaches obviate classical MOF assembly strategies, in which pre-designed building blocks are used to form specific, edge-transitive or highly regular topologies. Instead, they rely on methods such as transversal reticular chemistry; use of zigzag ligands; introduction of twisting into the ligand carboxylate groups; alteration of ligand bending angles; and changing of the length/width ratio in branched ligands. Thus, by combining classical topology with these techniques to create non-default geometry, researchers are gradually elucidating the pre-requisites for designing MOFs with complex topologies. As researchers have come to understand the basic rules for assembly of some of the topologies previously discovered serendipitously (*e.g.* **gea**, **sky**, **agw**, and **pek**), they have been able to exploit these topologies to further rationally design isoreticular materials. In several cases, the MBBs are left unsaturated, such that the aforementioned approaches to non-default topologies can be harnessed to construct multivariate MOFs with precisely-positioned functional groups, with the aim of creating functional sequences that mimicking natural structures such as enzymes or DNA. Finally, given the potential of geometry mismatch to generate countless new MOF topologies, we consider that human efforts to predict MOF topology are about to reach their limit. Accordingly, we believe that if the MOF research community truly wants to attain the next level of structural complexity in rational design, we must now turn to computational approaches to complement our human efforts. Clearly, such computational tools should be openly available and accessible to theoretical and experimental scientists in materials science, chemistry and related fields.

AUTHOR INFORMATION

Corresponding Author

* vincent.guillerm@icn2.cat, daniel.maspoch@icn2.cat

Author Contributions

All authors have given approval to the final version of the manuscript

Notes

In various cases, the topology used to design specific MOFs, or the reported topology, do not match those obtained by following the recommendations of O'Keeffe and coworkers, on using derived nets. For such cases, we have denoted both topologies in the text (*e.g.* **rht**/**ntt**, **ftw**/**kle**, **nbo**/**fof**, *etc.*).

In the case several crystallographically independent ligands are present in a structure, ranges of bend angle or average twist/torsion angle are reported in this review.

ACKNOWLEDGMENT

Dr. Volodymyr Bon and Dr. Feng Liang are acknowledged for their help regarding the signification of some topology acronyms. Borja Ortin-Rubio is acknowledged for his helpful comments on a preliminary version of the review.

ABBREVIATIONS

General acronyms (order of appearance): MOF, metal-organic framework; MBB, molecular building block; SBU, secondary building unit; IRMOF, isoreticular MOF; RCSR, reticular chemistry structure resource; SBB, supermolecular building block; RE, rare earth; MOP, metal-organic polyhedra; L-L, ligand-to-ligand; SBL, supermolecular building layer; DNA, deoxyribonucleic acid.

Materials acronyms (order of appearance): HKUST, Hong Kong University of Science and Technology; MOF, Metal-Organic Framework; MIL, Material Institute Lavoisier; UiO, Universitetet i Oslo; DUT, Dresden University of Technology; JLU, Jilin University; CAU, Christian Albrechts University; BUT, Beijing University of

Technology; MIP, Materials from Institute of porous materials of Paris; PCN, porous coordination network; UPC, University of Petroleum, Qingdao, China; UMCM, University of Michigan crystalline material; SNNU, Shangqiu Normal University; ZJU, Zhejiang University; NOTT, Nottingham; NU, Northwestern University; UTSA, the University of Texas at San Antonio.

Ligands acronyms (order of appearance): tcpp, tetrakis(4-carboxyphenyl)porphyrin; bdc, terephthalate; Br-bdc, bromo-terephthalate; Me_2bpdc, 2,2′-dimethyl biphenyl-4,4′-dicarboxylate; pdi, N,N′-di-(4-benzate)-1,2,6,7-tetrachloroperylene-3,4,9,10-tetracarboxylic acid diimide; fldc, 9- fluoreneone- 2,7- dicarboxylate; dttdc, dithienothiophene dicarboxylate; tadiba, 4,4'-(2 H-1,2,4-triazole-3,5-diyl) dibenzoate; tdc, 2,5-thiophenedicarboxylate; pzdc, 3,5-pyrazoledicarboxylate; fdc, 2,5-furandicarboxylic; *m*-bdc, isophthalate; bdb, 4,4'-(benzene-1,3-diyl)dibenzoate; ndb, 4,4'-(naphthalene-2,7-diyl)dibenzoate; *m*-bdc-F_4, tetrafluoroisophthalate; cdc, 9h-Carbazole-3,6-dicarboxylate; tmuc, *trans*, *trans* muconate; 26ndc, 2,6-naphthalene dicarboxylate; 22bipy44dc, 2 2'-bipyridine-4 4'-dicarboxylate; azo33, azobenzene-3 3'-dicarboxylate; suc, succinate; azo44, azobenzene-4 4'-dicarboxylate; 44bpdc, 4,4'-biphenyldicarboxylate; btb, 4,4′,4″,-benzene-1,3,5-triyl-trisbenzoate; bcdc, 9-(4-carboxyphenyl)-9H-carbazole-3,6-dicarboxylate; bptc, [1,1'-biphenyl]-3,4',5-tricarboxylate; obi, 5-(4-carboxybenzyloxy)isophthalate; tptc, [1,1':3',1"-terphenyl]-4,4",5'-tricarboxylate; btc, trimesate; tatb, 4,4′,4″-s-Triazine-2,4,6-triyl-tribenzoate; Me_3btb, 4,4',4''-(2,4,6-trimethyl-benzene-1,3,5-triyl)tribenzoate; tnna, 6,6′,6″-(2,4,6-trimethylbenzene-1,3,5-triyl)tris(2-naphthoate)); bbc, 4,4',4''-[benzene-1,3,5-triyl-tris(benzene-4,1-diyl)]tribenzoate; btba, 4,4′,4″-(1H-benzo[d]imidazole-2,4,7-triyl)tribenzoate; bte, 4,4',4''-[benzene-1,3,5-triyltris(ethyne-2,1-diyl)]tribenzoate; ittc, 4,4',4''-(1H-imidazole-2,4,5-triyl)tribenzoate; bpcdc, 4,4′-(9-(4′-carboxy-[1,1′-biphenyl]-4-yl)-9*H*-carbazole-3,6-diyl)dibenzoate; tca, 4,4',4"- tricarboxylate triphenylamine; btb-*m*NH_2, 1-(3-amino-4-carboxyphenyl)-3-(4-carboxyphenyl)-5-(4-carboxynaphthalen-1-yl)-benzene; btac, benzene-1,3,5-tri-β-acryate; bptet, biphenyl-3,3′,5,5′-tetracarboxylate; azotet, 3,3′,5,5′-azobenzene-tetracarboxylate; tptet, [1,1′:4′,1″]terphenyl- 3,3″,5,5″-tetracarboxylate; tpcb, 3,3',5,5'-tetra(ethyl-4-carboxyphenyl)-1,1'biphenyl; tcpb, 4,4',4",4"'-benzene-1,2,4,5-tetrayl-tetrabenzoate; bhb, ,3',3'',5,5',5''-benzene-1,3,5-triyl-hexabenzoate; lnu108, 1,3,5-tris[(1,3-di(4'-carboxylate-phenyl)-phenyl)-5-ethynyl]benzene; lgea2, 5′,5‴″-((5-((4-(3,6-dicarboxylato-9H-carbazol-9-yl)phenyl)ethynyl)-1,3-phenylene)bis(ethyne-2,1-diyl))bis((1,1′:3′,1″-terphenyl]-4,4″-dicarboxylate)

Topology acronyms (order of appearance): **rht**, rhombicuboctahedron, triangle; **ith**, icosahedron, tetrahedron; **ftw**, four, twelve; **shp**, square, hexagonal prism; **fcu**, face centered cubic; **sql**, square lattice; **nbo**, NbO; **cds**, CdS; **bcu**, body centered cubic; **dia**, diamond; **kgm**, Kagomé lattice; **reo**, ReO; **bon**, Volodymyr Bon; **hbr**, XXX; **bct**, body centered tetragonal; **kag**, Kagomé net; **pcu**, primitive cubic; **nht**, XXX; **gea**, Guillerm, Eddaoudi, net A; **aea**, Alezi, Eddaoudi, net A; **pek**, Puthan Peedikakkal, Eddaoudi, Kaust; **flg**, Feng Liang; **ytw**, Yutong Wang; **sep**, september; **csq**, cube, square; **spn**, spinel; **kgd**, Kagomé dual; **the**, three, eight; **llj**, XXX; **sky**, XXX; **tbo**, twisted boracite; **agw**, AgW; **fmj**, XXX; **gee**, Guillerm, Eddaoudi, net E; **ceq**, XXX, **dag**, XXX; **hwx**, XXX, **sit**, XXX; **ydq**, XXX; **moo**, MIL-100; **mtn**, MTN zeolite type; **fmz**, Feng Ming Zhang; **pyr**, pyrite; **qom**, Queen of MOFs; **rtl**, rutile; **fof**, XXX, **ssa**, square, square, net A, **sty**, square, triangles axis Y; **ssb**, square, square, net B; **stx**, , square, triangles axis X; **lvt**, lattice complex ^{v}T; **lil**, XXX; **pts**, PtS; **tfk**, XXX; **tfb**, XXX; **she**, square, hexagon; **scu**, square, cube; **flu**, fluorite; **sqc**, square, cube; **stp**, square, trigonal prism; **kle**, Kaust, Luebke, Eddaoudi; **lim**, XXX; **tty**, XXX; **xly**, XXX; **xlz**, XXX; **cut**, cube, triangle; **flt**, fluorite, triangle **ntt**, Nottingham; **zyg**, Zhiyong Guo; **gwe**, Guillerm, Weseliński, Eddaoudi.

We could not identify the correspondence for the following topology acronyms: **hbr**, **nht**, **llj**, **sky**, **fmj**, **ceq**, **dag**, **hwx**, **sit**, **ydq**, **fof**, **lil**, **tfk**, **tfb**, **lim**, **tty**, **xly**, **xlz**.

REFERENCES

1. S. S. Y. Chui, S. M. F. Lo, J. P. H. Charmant, A. G. Orpen and I. D. Williams, *Science*, 1999, **283**, 1148-1150.
2. H. Li, M. Eddaoudi, M. O'Keeffe and O. M. Yaghi, *Nature*, 1999, **402**, 276-279.
3. H. Furukawa, K. E. Cordova, M. O'Keeffe and O. M. Yaghi, *Science*, 2013, **341**.
4. V. Guillerm, D. Kim, J. F. Eubank, R. Luebke, X. Liu, K. Adil, M. S. Lah and M. Eddaoudi, *Chem. Soc. Rev.*, 2014, **43**, 6141-6172.
5. S. Subramanian and M. J. Zaworotko, *Angew. Chem., Int. Ed.*, 1995, **34**, 2127-2129.
6. M. O'Keeffe, M. Eddaoudi, H. L. Li, T. M. Reineke and O. M. Yaghi, *J. Solid State Chem.*, 2000, **152**, 3-20.

7. M. Eddaoudi, D. B. Moler, H. L. Li, B. L. Chen, T. M. Reineke, M. O'Keeffe and O. M. Yaghi, *Acc. Chem. Res.*, 2001, **34**, 319-330.

8. O. M. Yaghi, M. O'Keeffe, N. W. Ockwig, H. K. Chae, M. Eddaoudi and J. Kim, *Nature*, 2003, **423**, 705-714.

9. H. Jiang, J. Jia, A. Shkurenko, Z. Chen, K. Adil, Y. Belmabkhout, L. J. Weselinski, A. H. Assen, D.-X. Xue, M. O'Keeffe and M. Eddaoudi, *J. Am. Chem. Soc.*, 2018, **140**, 8858-8867.

10. D. J. Tranchemontagne, J. L. Mendoza-Cortes, M. O'Keeffe and O. M. Yaghi, *Chem. Soc. Rev.*, 2009, **38**, 1257-1283.

11. O. Delgado-Friedrichs, M. O'Keeffe and O. M. Yaghi, *Acta Cryst. A*, 2006, **62**, 350-355.

12. O. Delgado-Friedrichs and M. O'Keeffe, *Acta Cryst. A*, 2007, **63**, 344-347.

13. M. Li, D. Li, M. O'Keeffe and O. M. Yaghi, *Chem. Rev.*, 2014, **114**, 1343-1370.

14. M. O'Keeffe and O. M. Yaghi, *Chem. Rev.*, 2012, **112**, 675-702.

15. Y. Belmabkhout, V. Guillerm and M. Eddaoudi, *Chem. Eng. J.*, 2016, **296**, 386-397.

16. H. Mouttaki, Y. Belmabkhout, J. F. Eubank, V. Guillerm and M. Eddaoudi, *RSC Adv.*, 2014, DOI: 10.1039/C4RA12432D.

17. O. Shekhah, Y. Belmabkhout, Z. Chen, V. Guillerm, A. Cairns, K. Adil and M. Eddaoudi, *Nat. Commun.*, 2014, **5**, 4228.

18. H. Li, K. Wang, Y. Sun, C. T. Lollar, J. Li and H.-C. Zhou, *Materials Today*, 2018, **21**, 108-121.

19. J. Li, X. Wang, G. Zhao, C. Chen, Z. Chai, A. Alsaedi, T. Hayat and X. Wang, *Chem. Soc. Rev.*, 2018, **47**, 2322-2356.

20. D. T. Sun, N. Gasilova, S. Yang, E. Oveisi and W. L. Queen, *J. Am. Chem. Soc.*, 2018, **140**, 16697-16703.

21. H. Kim, S. R. Rao, E. A. Kapustin, L. Zhao, S. Yang, O. M. Yaghi and E. N. Wang, *Nat. Commun.*, 2018, **9**, 1191.

22. H. Kim, S. Yang, S. R. Rao, S. Narayanan, E. A. Kapustin, H. Furukawa, A. S. Umans, O. M. Yaghi and E. N. Wang, *Science*, 2017, **356**, 430-434.

23. M. J. Kalmutzki, C. S. Diercks and O. M. Yaghi, *Advanced Materials*, 2018, **30**, 1704304.

24. L. Garzón-Tovar, J. Pérez-Carvajal, I. Imaz and D. Maspoch, *Adv. Funct. Mater.*, 2017, **27**, 1606424.

25. H. Furukawa, F. Gándara, Y.-B. Zhang, J. Jiang, W. L. Queen, M. R. Hudson and O. M. Yaghi, *J. Am. Chem. Soc.*, 2014, **136**, 4369-4381.

26. J. Troyano, A. Carné-Sánchez, J. Pérez-Carvajal, L. León-Reina, I. Imaz, A. Cabeza and D. Maspoch, *Angew. Chem., Int. Ed.*, 2018, **57**, 15420-15424.

27. X. Wang, X.-Z. Chen, C. C. J. Alcântara, S. Sevim, M. Hoop, A. Terzopoulou, C. de Marco, C. Hu, A. J. de Mello, P. Falcaro, S. Furukawa, B. J. Nelson, J. Puigmartí-Luis and S. Pané, *Advanced Materials*, **0**, 1901592.

28. J. Troyano, A. Carné-Sánchez and D. Maspoch, *Advanced Materials*, 2019, **31**, 1808235.

29. M. O'Keeffe, M. A. Peskov, S. J. Ramsden and O. M. Yaghi, *Acc. Chem. Res.*, 2008, **41**, 1782-1789.

30. P. Z. Moghadam, A. Li, S. B. Wiggin, A. Tao, A. G. P. Maloney, P. A. Wood, S. C. Ward and D. Fairen-Jimenez, *Chem. Mater.*, 2017, **29**, 2618-2625.

31. M. Eddaoudi, *Unpublished results*.

32. V. Guillerm, Ł. J. Weseliński, Y. Belmabkhout, A. J. Cairns, V. D'Elia, Ł. Wojtas, K. Adil and M. Eddaoudi, *Nat. Chem.*, 2014, **6**, 673-680.

33. S. Yuan, J.-S. Qin, C. T. Lollar and H.-C. Zhou, *ACS Central Science*, 2018, **4**, 440-450.

34. D. Alezi, A. M. P. Peedikakkal, Ł. J. Weseliński, V. Guillerm, Y. Belmabkhout, A. J. Cairns, Z. Chen, Ł. Wojtas and M. Eddaoudi, *J. Am. Chem. Soc.*, 2015, **137**, 5421-5430.

35. D. Feng, H.-L. Jiang, Y.-P. Chen, Z.-Y. Gu, Z. Wei and H.-C. Zhou, *Inorg. Chem.*, 2013, **52**, 12661-12667.

36. H. Furukawa, J. Kim, N. W. Ockwig, M. O'Keeffe and O. M. Yaghi, *J. Am. Chem. Soc.*, 2008, **130**, 11650-11661.

37. M. Eddaoudi, J. Kim, D. Vodak, A. Sudik, J. Wachter, M. O'Keeffe and O. M. Yaghi, *Proc. Nat. Acad. Sci. USA*, 2002, **99**, 4900-4904.

38. http://europe.iza-structure.org/IZA-SC/ftc_table.php, (accessed 05/06/2019).

39. F. Nouar, J. F. Eubank, T. Bousquet, Ł. Wojtas, M. J. Zaworotko and M. Eddaoudi, *J. Am. Chem. Soc.*, 2008, **130**, 1833-1834.

40. V. Guillerm, S. Gross, C. Serre, T. Devic, M. Bauer and G. Férey, *Chem. Commun.*, 2010, **46**, 767-769.

41. M. Dan-Hardi, C. Serre, T. Frot, L. Rozes, G. Maurin, C. Sanchez and G. Férey, *J. Am. Chem. Soc.*, 2009, **131**, 10857-10859.

42. D.-X. Xue, A. J. Cairns, Y. Belmabkhout, Ł. Wojtas, Y. Liu, M. H. Alkordi and M. Eddaoudi, *J. Am. Chem. Soc.*, 2013, **135**, 7660-7667.

43. Y. Wang, L. Feng, W. Fan, K.-Y. Wang, X. Wang, X. Wang, K. Zhang, X. Zhang, F. Dai, D. Sun and H.-C. Zhou, *J. Am. Chem. Soc.*, 2019, **141**, 6967-6975.

44. T. Ahnfeldt, N. Guillou, D. Gunzelmann, I. Margiolaki, T. Loiseau, G. Férey, J. Senker and N. Stock, *Angew. Chem., Int. Ed.*, 2009, **48**, 5163-5166.

45. N. M. Padial, E. Quartapelle Procopio, C. Montoro, E. López, J. E. Oltra, V. Colombo, A. Maspero, N. Masciocchi, S. Galli, I. Senkovska, S. Kaskel, E. Barea and J. A. R. Navarro, *Angew. Chem., Int. Ed.*, 2013, **52**, 8290-8294.

46. D.-Y. Du, J.-S. Qin, Z. Sun, L.-K. Yan, M. O'Keeffe, Z.-M. Su, S.-L. Li, X.-H. Wang, X.-L. Wang and Y.-Q. Lan, *Sci. Rep.*, 2013, **3**, 2616.

47. J. F. Eubank, F. Nouar, R. Luebke, A. J. Cairns, Ł. Wojtas, M. Alkordi, T. Bousquet, M. R. Hight, J. Eckert, J. P. Embs, P. A. Georgiev and M. Eddaoudi, *Angew. Chem., Int. Ed.*, 2012, **51**, 10099-10103.

48. U. Stoeck, S. Krause, V. Bon, I. Senkovska and S. Kaskel, *Chem. Commun.*, 2012, **48**, 10841-10843.

49. M. Eddaoudi, J. Kim, M. O'Keeffe and O. M. Yaghi, *J. Am. Chem. Soc.*, 2002, **124**, 376-377.

50. V. Guillerm, T. Grancha, I. Imaz, J. Juanhuix and D. Maspoch, *J. Am. Chem. Soc.*, 2018, **140**, 10153-10157.

51. C. R. Groom, I. J. Bruno, M. P. Lightfoot and S. C. Ward, *Acta Cryst. B*, 2016, **72**, 171-179.

52. G. Férey, C. Serre, C. Mellot-Draznieks, F. Millange, S. Surblé, J. Dutour and I. Margiolaki, *Angew. Chem., Int. Ed.*, 2004, **43**, 6296-6301.

53. J. H. Cavka, S. Jakobsen, U. Olsbye, N. Guillou, C. Lamberti, S. Bordiga and K. P. Lillerud, *J. Am. Chem. Soc.*, 2008, **130**, 13850-13851.

54. O. Delgado Friedrichs, M. O'Keeffe and O. M. Yaghi, *Acta Cryst. A*, 2003, **59**, 515-525.

55. O. Delgado Friedrichs, M. O'Keeffe and O. M. Yaghi, *Acta Cryst. A*, 2003, **59**, 22-27.

56. O. Delgado-Friedrichs, M. D. Foster, M. O'Keeffe, D. M. Proserpio, M. M. J. Treacy and O. M. Yaghi, *J. Solid State Chem.*, 2005, **178**, 2533-2554.

57. O. Delgado-Friedrichs, M. O'Keeffe and O. M. Yaghi, *Phys. Chem. Chem. Phys.*, 2007, **9**, 1035-1043.

58. W. Morris, B. Volosskiy, S. Demir, F. Gándara, P. L. McGrier, H. Furukawa, D. Cascio, J. F. Stoddart and O. M. Yaghi, *Inorg. Chem.*, 2012, **51**, 6443-6445.

59. M. Eddaoudi, J. Kim, N. Rosi, D. Vodak, J. Wachter, M. O'Keeffe and O. M. Yaghi, *Science*, 2002, **295**, 469-472.

60. B. F. Abrahams, S. R. Batten, H. Hamit, B. F. Hoskins and R. Robson, *Angew. Chem., Int. Ed.*, 1996, **35**, 1690-1692.

61. W. Mori, F. Inoue, K. Yoshida, H. Nakayama, S. Takamizawa and M. Kishita, *Chem. Letters*, 1997, **26**, 1219-1220.

62. O. M. Yaghi, C. E. Davis, G. Li and H. Li, *J. Am. Chem. Soc.*, 1997, **119**, 2861-2868.

63. H. Li, M. Eddaoudi, T. L. Groy and O. M. Yaghi, *J. Am. Chem. Soc.*, 1998, **120**, 8571-8572.

64. B. Chen, M. Eddaoudi, S. T. Hyde, M. O'Keeffe and O. M. Yaghi, *Science*, 2001, **291**, 1021-1023.

65. S. Yuan, Y.-P. Chen, J.-S. Qin, W. Lu, L. Zou, Q. Zhang, X. Wang, X. Sun and H.-C. Zhou, *J. Am. Chem. Soc.*, 2016, **138**, 8912-8919.

66. S. Yuan, L. Zou, H. Li, Y. P. Chen, J. Qin, Q. Zhang, W. Lu, M. B. Hall and H. C. Zhou, *Angew. Chem., Int. Ed.*, 2016, **55**, 10776-10780.

67. C. X. Chen, Z. Wei, J. J. Jiang, Y. Z. Fan, S. P. Zheng, C. C. Cao, Y. H. Li, D. Fenske and C. Y. Su, *Angew. Chem., Int. Ed.*, 2016, **55**, 9932-9936.

68. Q. Yang, A. D. Wiersum, P. L. Llewellyn, V. Guillerm, C. Serred and G. Maurin, *Chem. Commun.*, 2011, **47**, 9603-9605.

69. Q. Yang, V. Guillerm, F. Ragon, A. D. Wiersum, P. L. Llewellyn, C. Zhong, T. Devic, C. Serre and G. Maurin, *Chem. Commun.*, 2012, **48**, 9831-9833.

70. O. V. Gutov, S. Molina, E. C. Escudero- Adán and A. Shafir, *Chem. Eur. J.*, 2016, **22**, 13582-13587.

71. R. J. Marshall, C. L. Hobday, C. F. Murphie, S. L. Griffin, C. A. Morrison, S. A. Moggach and R. S. Forgan, *J. Mater. Chem. A*, 2016, **4**, 6955-6963.

72. B. Lü, Y. Chen, P. Li, B. Wang, K. Müllen and M. Yin, *Nat. Commun.*, 2019, **10**, 767.

73. M. Eddaoudi, J. Kim, J. B. Wachter, H. K. Chae, M. O'Keeffe and O. M. Yaghi, *J. Am. Chem. Soc.*, 2001, **123**, 4368-4369.

74. H. Abourahma, A. W. Coleman, B. Moulton, B. Rather, P. Shahgaldian and M. J. Zaworotko, *Chem. Commun.*, 2001, DOI: 10.1039/b106592k, 2380-2381.

75. J. J. I. V. Perry, J. A. Perman and M. J. Zaworotko, *Chem. Soc. Rev.*, 2009, **38**, 1400-1417.

76. R. Chakrabarty, P. S. Mukherjee and P. J. Stang, *Chem. Rev.*, 2011, **111**, 6810-6918.

77. T. R. Cook, Y.-R. Zheng and P. J. Stang, *Chem. Rev.*, 2013, **113**, 734-777.

78. D. J. Tranchemontagne, Z. Ni, M. O'Keeffe and O. M. Yaghi, *Angew. Chem., Int. Ed.*, 2008, **47**, 5136-5147.

79. J.-R. Li, A. A. Yakovenko, W. Lu, D. J. Timmons, W. Zhuang, D. Yuan and H.-C. Zhou, *J. Am. Chem. Soc.*, 2010, **132**, 17599-17610.

80. D. Fujita, Y. Ueda, S. Sato, N. Mizuno, T. Kumasaka and M. Fujita, *Nature*, 2016, **540**, 563.

81. F. Drache, V. Bon, I. Senkovska, M. Adam, A. Eychmüller and S. Kaskel, *Eur. J. Inorg. Chem.*, 2016, **2016**, 4483-4489.

82. V. Bon, V. Senkovskyy, I. Senkovska and S. Kaskel, *Chem. Commun.*, 2012, **48**, 8407-8409.

83. X. Sun, J. Gu, Y. Yuan, C. Yu, J. Li, H. Shan, G. Li and Y. Liu, *Inorg. Chem.*, 2019, **58**, 7480-7487.

84. V. Bon, I. Senkovska, I. A. Baburin and S. Kaskel, *Cryst. Growth Des.*, 2013, **13**, 1231-1237.

85. F. Drache, V. Bon, I. Senkovska, J. Getzschmann and S. Kaskel, *Phil. Trans. R. Soc. A*, 2017, **375**, 20160027.

86. A. C. Dreischarf, M. Lammert, N. Stock and H. Reinsch, *Inorg. Chem.*, 2017, **56**, 2270-2277.

87. L.-H. Xie, X.-M. Liu, T. He and J.-R. Li, *Chem*, 2018, **4**, 1911-1927.

88. W. Wei, X. Wang, K. Zhang, C.-B. Tian and S.-W. Du, *Cryst. Growth Des.*, 2019, **19**, 55-59.

89. S. Krause, V. Bon, U. Stoeck, I. Senkovska, D. M. Többens, D. Wallacher and S. Kaskel, *Angew. Chem., Int. Ed.*, 2017, **56**, 10676-10680.

90. P. Szuromi, *Science*, 2018, **361**, 889-890.

91. Z.-F. Chen, Z.-L. Zhang, Y.-H. Tan, Y.-Z. Tang, H.-K. Fun, Z.-Y. Zhou, B. F. Abrahams and H. Liang, *CrystEngComm*, 2008, **10**, 217-231.

92. X.-S. Wang, S. Ma, K. Rauch, J. M. Simmons, D. Yuan, X. Wang, T. Yildirim, W. C. Cole, J. J. Lopez, A. de Meijere and H.-C. Zhou, *Chem. Mater.*, 2008, **20**, 3145-3152.

93. H.-C. Kim, S. Huh, S.-J. Kim and Y. Kim, *Scientific Reports*, 2017, **7**, 17185.

94. M. Wahiduzzaman, S. Wang, B. J. Sikora, C. Serre and G. Maurin, *Chem. Commun.*, 2018, **54**, 10812-10815.

95. H. T. T. Nguyen, T. N. Tu, M. V. Nguyen, T. H. N. Lo, H. Furukawa, N. N. Nguyen and M. D. Nguyen, *ACS Applied Materials & Interfaces*, 2018, **10**, 35462-35468.

96. V. Guillerm, F. Ragon, M. Dan-Hardi, T. Devic, M. Vishnuvarthan, B. Campo, A. Vimont, G. Clet, Q. Yang, G. Maurin, G. Férey, A. Vittadini, S. Gross and C. Serre, *Angew. Chem., Int. Ed.*, 2012, **51**, 9267-9271.

97. V. Guillerm, H. Xu, J. Albalad, I. Imaz and D. Maspoch, *J. Am. Chem. Soc.*, 2018, **140**, 15022-15030.

98. S. Yuan, L. Zou, J.-S. Qin, J. Li, L. Huang, L. Feng, X. Wang, M. Bosch, A. Alsalme, T. Cagin and H.-C. Zhou, *Nat. Commun.*, 2017, **8**, 15356.

99. H. Chevreau, T. Devic, F. Salles, G. Maurin, N. Stock and C. Serre, *Angew. Chem., Int. Ed.*, 2013, **52**, 5056-5060.

100. B. D. N. and D. W. R., *Chem. Eur. J.*, 2013, **19**, 818-827.

101. A. P. Nelson, D. A. Parrish, L. R. Cambrea, L. C. Baldwin, N. J. Trivedi, K. L. Mulfort, O. K. Farha and J. T. Hupp, *Cryst. Growth Des.*, 2009, **9**, 4588-4591.

102. J. Li, Y. Peng, H. Liang, Y. Yu, B. Xin, G. Li, Z. Shi and S. Feng, *Eur. J. Inorg. Chem.*, 2011, **2011**, 2712-2719.

103. H. Deng, C. J. Doonan, H. Furukawa, R. B. Ferreira, J. Towne, C. B. Knobler, B. Wang and O. M. Yaghi, *Science*, 2010, **327**, 846-850.

104. K. Koh, A. G. Wong-Foy and A. J. Matzger, *Angew. Chem., Int. Ed.*, 2008, **47**, 677-680.

105. K. Koh, A. G. Wong-Foy and A. J. Matzger, *J. Am. Chem. Soc.*, 2009, **131**, 4184-4185.

106. Q.-G. Zhai, X. Bu, X. Zhao, D.-S. Li and P. Feng, *Acc. Chem. Res.*, 2017, **50**, 407-417.

107. L. Liu, K. Konstas, M. R. Hill and S. G. Telfer, *J. Am. Chem. Soc.*, 2013, **135**, 17731-17734.

108. H. Kim, D. Kim, D. Moon, Y. N. Choi, S. B. Baek and M. S. Lah, *Chem. Sci.*, 2019, DOI: 10.1039/C9SC01301F.

109. T. T. M. Nguyen, H. M. Le, Y. Kawazoe and H. L. Nguyen, *Materials Chemistry Frontiers*, 2018, **2**, 2063-2069.

110. T. He, Y.-Z. Zhang, X.-J. Kong, J. Yu, X.-L. Lv, Y. Wu, Z.-J. Guo and J.-R. Li, *ACS Applied Materials & Interfaces*, 2018, **10**, 16650-16659.

111. G. Kickelbick and U. Schubert, *Chemische Berichte*, 1997, **130**, 473-478.

112. A. Otero, J. Fernández-Baeza, A. Antiñolo, J. Tejeda, A. Lara-Sánchez, L. Sánchez-Barba, M. Fernández-López and I. López-Solera, *Inorg. Chem.*, 2004, **43**, 1350-1358.

113. A. Schaate, P. Roy, A. Godt, J. Lippke, F. Waltz, M. Wiebcke and P. Behrens, *Chem. Eur. J.*, 2011, **17**, 6643-6651.

114. F.-X. Coudert, https://twitter.com/MOF_papers/status/1071974578400845824).

115. Z. Chen, S. L. Hanna, L. R. Redfern, D. Alezi, T. Islamoglu and O. K. Farha, *Coordination Chemistry Reviews*, 2019, **386**, 32-49.

116. Y. Bai, Y. Dou, L.-H. Xie, W. Rutledge, J.-R. Li and H.-C. Zhou, *Chem. Soc. Rev.*, 2016, **45**, 2327-2367.

117. D. Feng, K. Wang, J. Su, T.-F. Liu, J. Park, Z. Wei, M. Bosch, A. Yakovenko, X. Zou and H.-C. Zhou, *Angew. Chem., Int. Ed.*, 2015, **54**, 149-154.

118. R. Wang, Z. Wang, Y. Xu, F. Dai, L. Zhang and D. Sun, *Inorg. Chem.*, 2014, **53**, 7086-7088.

119. B. Wang, X.-L. Lv, D. Feng, L.-H. Xie, J. Zhang, M. Li, Y. Xie, J.-R. Li and H.-C. Zhou, *J. Am. Chem. Soc.*, 2016, **138**, 6204-6216.

120. S. Lee, H.-B. Bürgi, S. A. Alshmimri and O. M. Yaghi, *J. Am. Chem. Soc.*, 2018, **140**, 8958-8964.

121. B. Guo, F. Li, C. Wang, L. Zhang and D. Sun, *J. Mater. Chem. A*, 2019, DOI: 10.1039/C9TA03126J.

122. H. Furukawa, Y. B. Go, N. Ko, Y. K. Park, F. J. Uribe-Romo, J. Kim, M. O'Keeffe and O. M. Yaghi, *Inorg. Chem.*, 2011, **50**, 9147-9152.

123. D. Sun, S. Ma, Y. Ke, D. J. Collins and H.-C. Zhou, *J. Am. Chem. Soc.*, 2006, **128**, 3896-3897.

124. A. G. Wong-Foy, O. Lebel and A. J. Matzger, *J. Am. Chem. Soc.*, 2007, **129**, 15740-15741.

125. C.-S. Lim, J. K. Schnobrich, A. G. Wong-Foy and A. J. Matzger, *Inorg. Chem.*, 2010, **49**, 5271-5275.

126. Z. Lu, L. Du, B. Zheng, J. Bai, M. Zhang and R. Yun, *CrystEngComm*, 2013, **15**, 9348-9351.

127. J. K. Schnobrich, O. Lebel, K. A. Cychosz, A. Dailly, A. G. Wong-Foy and A. J. Matzger, *J. Am. Chem. Soc.*, 2010, **132**, 13941-13948.

128. U. Stoeck, I. Senkovska, V. Bon, S. Krause and S. Kaskel, *Chem. Commun.*, 2015, **51**, 1046-1049.

129. J.-R. Li, D. J. Timmons and H.-C. Zhou, *J. Am. Chem. Soc.*, 2009, **131**, 6368-6369.

130. C. Mellot-Draznieks, J. Dutour and G. Férey, *Z. Anorg. Allg. Chem.*, 2004, **630**, 2599-2604.

131. C. Mellot-Draznieks, J. Dutour and G. Férey, *Angewandte Chemie*, 2004, **116**, 6450-6456.

132. P. Horcajada, H. Chevreau, D. Heurtaux, F. Benyettou, F. Salles, T. Devic, A. Garcia-Marquez, C. Yu, H. Lavrard, C. L. Dutson, E. Magnier, G. Maurin, E. Elkaïm and C. Serre, *Chem. Commun.*, 2014, **50**, 6872-6874.

133. D. Feng, T.-F. Liu, J. Su, M. Bosch, Z. Wei, W. Wan, D. Yuan, Y.-P. Chen, X. Wang, K. Wang, X. Lian, Z.-Y. Gu, J. Park, X. Zou and H.-C. Zhou, *Nat. Commun.*, 2015, **6**, 5979.

134. X. Lian, Y.-P. Chen, T.-F. Liu and H.-C. Zhou, *Chem. Sci.*, 2016, **7**, 6969-6973.

135. I. A. Ibarra, X. Lin, S. Yang, A. J. Blake, G. S. Walker, S. A. Barnett, D. R. Allan, N. R. Champness, P. Hubberstey and M. Schröder, *Chem. Eur. J.*, 2010, **16**, 13671-13679.

136. H. K. Chae, D. Y. Siberio-Perez, J. Kim, Y. Go, M. Eddaoudi, A. J. Matzger, M. O'Keeffe and O. M. Yaghi, *Nature*, 2004, **427**, 523-527.

137. D. Feng, K. Wang, Z. Wei, Y.-P. Chen, C. M. Simon, R. K. Arvapally, R. L. Martin, M. Bosch, T.-F. Liu, S. Fordham, D. Yuan, M. A. Omary, M. Haranczyk, B. Smit and H.-C. Zhou, *Nat. Commun.*, 2014, **5**, 5723.

138. J.-W. Zhang, W.-J. Ji, M.-C. Hu, S.-N. Li, Y.-C. Jiang, X.-M. Zhang, P. Qu and Q.-G. Zhai, *Inorganic Chemistry Frontiers*, 2019, **6**, 813-819.

139. F.-M. Zhang, L.-Z. Dong, J.-S. Qin, W. Guan, J. Liu, S.-L. Li, M. Lu, Y.-Q. Lan, Z.-M. Su and H.-C. Zhou, *J. Am. Chem. Soc.*, 2017, **139**, 6183-6189.

140. H. K. Chae, J. Kim, O. D. Friedrichs, M. O'Keeffe and O. M. Yaghi, *Angew. Chem., Int. Ed.*, 2003, **42**, 3907-3909.

141. Y.-B. Zhang, H. Furukawa, N. Ko, W. Nie, H. J. Park, S. Okajima, K. E. Cordova, H. Deng, J. Kim and O. M. Yaghi, *J. Am. Chem. Soc.*, 2015, **137**, 2641-2650.

142. J. Jiang, H. Furukawa, Y.-B. Zhang and O. M. Yaghi, *J. Am. Chem. Soc.*, 2016, **138**, 10244-10251.

143. H. Furukawa, N. Ko, Y. B. Go, N. Aratani, S. B. Choi, E. Choi, A. Ö. Yazaydin, R. Q. Snurr, M. O'Keeffe, J. Kim and O. M. Yaghi, *Science*, 2010, **329**, 424-428.

144. A. Verma, D. De, K. Tomar and P. K. Bharadwaj, *Inorg. Chem.*, 2017, **56**, 9765-9771.

145. W. Fan, Y. Wang, Z. Xiao, L. Zhang, Y. Gong, F. Dai, R. Wang and D. Sun, *Inorg. Chem.*, 2017, **56**, 13634-13637.

146. L. Kong, R. Zou, W. Bi, R. Zhong, W. Mu, J. Liu, R. P. S. Han and R. Zou, *J. Mater. Chem. A*, 2014, **2**, 17771-17778.

147. B. L. Chen, N. W. Ockwig, F. R. Fronczek, D. S. Contreras and O. M. Yaghi, *Inorg. Chem.*, 2005, **44**, 181-183.

148. Y. He, B. Li, M. O'Keeffe and B. Chen, *Chem. Soc. Rev.*, 2014, **43**, 5618-5656.

149. W. Lu, Z. Wei, Z.-Y. Gu, T.-F. Liu, J. Park, J. Park, J. Tian, M. Zhang, Q. Zhang, T. Gentle Iii, M. Bosch and H.-C. Zhou, *Chem. Soc. Rev.*, 2014, DOI: 10.1039/C4CS00003J.

150. X.-S. Wang, S. Ma, P. M. Forster, D. Yuan, J. Eckert, J. J. López, B. J. Murphy, J. B. Parise and H.-C. Zhou, *Angew. Chem., Int. Ed.*, 2008, **47**, 7263-7266.

151. X. Duan, J. Yu, J. Cai, Y. He, C. Wu, W. Zhou, T. Yildirim, Z. Zhang, S. Xiang, M. O'Keeffe, B. Chen and G. Qian, *Chem. Commun.*, 2013, **49**, 2043-2045.

152. X. Lin, I. Telepeni, A. J. Blake, A. Dailly, C. M. Brown, J. M. Simmons, M. Zoppi, G. S. Walker, K. M. Thomas, T. J. Mays, P. Hubberstey, N. R. Champness and M. Schroeder, *J. Am. Chem. Soc.*, 2009, **131**, 2159-2171.

153. R. Grünker, I. Senkovska, R. Biedermann, N. Klein, A. Klausch, I. A. Baburin, U. Mueller and S. Kaskel, *Eur. J. Inorg. Chem.*, 2010, **2010**, 3835-3841.

154. D. Sun, Y. Ke, T. M. Mattox, B. A. Ooro and H.-C. Zhou, *Chem. Commun.*, 2005, DOI: 10.1039/B505664K, 5447-5449.

155. D. Sun, D. J. Collins, Y. Ke, J.-L. Zuo and H.-C. Zhou, *Chem. Eur. J.*, 2006, **12**, 3768-3776.

156. W. Lu, D. Yuan, T. A. Makal, Z. Wei, J.-R. Li and H.-C. Zhou, *Dalton Trans.*, 2013, **42**, 1708-1714.

157. S. Krause, V. Bon, I. Senkovska, U. Stoeck, D. Wallacher, D. M. Többens, S. Zander, R. S. Pillai, G. Maurin, F.-X. Coudert and S. Kaskel, *Nature*, 2016, **532**, 348.

158. D. Feng, W.-C. Chung, Z. Wei, Z.-Y. Gu, H.-L. Jiang, Y.-P. Chen, D. J. Darensbourg and H.-C. Zhou, *J. Am. Chem. Soc.*, 2013, **135**, 17105-17110.

159. C.-W. Kung, T. C. Wang, J. E. Mondloch, D. Fairen-Jimenez, D. M. Gardner, W. Bury, J. M. Klingsporn, J. C. Barnes, R. Van Duyne, J. F. Stoddart, M. R. Wasielewski, O. K. Farha and J. T. Hupp, *Chem. Mater.*, 2013, **25**, 5012-5017.

160. D. Feng, Z.-Y. Gu, Y.-P. Chen, J. Park, Z. Wei, Y. Sun, M. Bosch, S. Yuan and H.-C. Zhou, *J. Am. Chem. Soc.*, 2014, **136**, 17714-17717.

161. H.-L. Jiang, D. Feng, K. Wang, Z.-Y. Gu, Z. Wei, Y.-P. Chen and H.-C. Zhou, *J. Am. Chem. Soc.*, 2013, **135**, 13934-13938.

162. P. T. K. Nguyen, H. T. D. Nguyen, H. N. Nguyen, C. A. Trickett, Q. T. Ton, E. Gutiérrez-Puebla, M. A. Monge, K. E. Cordova and F. Gándara, *ACS Applied Materials & Interfaces*, 2018, **10**, 733-744.

163. H. Wang, X. Dong, J. Lin, S. J. Teat, S. Jensen, J. Cure, E. V. Alexandrov, Q. Xia, K. Tan, Q. Wang, D. H. Olson, D. M. Proserpio, Y. J. Chabal, T. Thonhauser, J. Sun, Y. Han and J. Li, *Nat. Commun.*, 2018, **9**, 1745.

164. R. Luebke, Y. Belmabkhout, Ł. J. Weseliński, A. J. Cairns, M. Alkordi, G. Norton, Ł. Wojtas, K. Adil and M. Eddaoudi, *Chem. Sci.*, 2015, **6**, 4095-4102.

165. J. Pang, S. Yuan, J. Qin, C. Liu, C. Lollar, M. Wu, D. Yuan, H.-C. Zhou and M. Hong, *J. Am. Chem. Soc.*, 2017, **139**, 16939-16945.

166. M. Lammert, H. Reinsch, C. A. Murray, M. T. Wharmby, H. Terraschke and N. Stock, *Dalton Trans.*, 2016, **45**, 18822-18826.

167. J. Lyu, X. Zhang, K.-i. Otake, X. Wang, P. Li, Z. Li, Z. Chen, Y. Zhang, M. C. Wasson, Y. Yang, P. Bai, X. Guo, T. Islamoglu and O. K. Farha, *Chem. Sci.*, 2019, **10**, 1186-1192.

168. Y. Zou, M. Park, S. Hong and M. S. Lah, *Chem. Commun.*, 2008, DOI: 10.1039/B801103F, 2340-2342.

169. R. Luebke, J. F. Eubank, A. J. Cairns, Y. Belmabkhout, Ł. Wojtas and M. Eddaoudi, *Chem. Commun.*, 2012, **48**, 1455-1457.

170. O. K. Farha, I. Eryazici, N. C. Jeong, B. G. Hauser, C. E. Wilmer, A. A. Sarjeant, R. Q. Snurr, S. T. Nguyen, A. Ö. Yazaydın and J. T. Hupp, *J. Am. Chem. Soc.*, 2012, **134**, 15016-15021.

171. D. Zhao, D. Yuan, D. Sun and H.-C. Zhou, *J. Am. Chem. Soc.*, 2009, **131**, 9186-9187.

172. Z. Guo, H. Wu, G. Srinivas, Y. Zhou, S. Xiang, Z. Chen, Y. Yang, W. Zhou, M. O'Keeffe and B. Chen, *Angew. Chem., Int. Ed.*, 2011, **50**, 3178-3181.

173. J.-R. Li and H.-C. Zhou, *Angew. Chem., Int. Ed.*, 2009, **48**, 8465-8468.